MAX-PLANCK-GESELLSCHAFT

Max-Planck-Institut für Physik
(Werner-Heisenberg-Institut)

SEARCHING FOR DARK MATTER AXIONS WITH MADMAX

XIAOYUE LI

XYLI@MPP.MPG.DE

MAX PLANCK INSTITUTE FOR PHYSICS, MUNICH, GERMANY

13TH TERASCALE DETECTOR WORKSHOP, DESY

APR. 8, 2021

THE STRONG CP PROBLEM AND THE PECCEI-QUINN MECHANISM

- The QCD Lagrangian contains a CP-violating term:

$$\mathscr{L}_{QCD} = \ldots + \frac{\alpha_s}{8\pi}\,\bar{\theta}\,G_{\mu\nu a}\tilde{G}^{\mu\nu}_a,$$
$$\bar{\theta} = \theta_{QCD} + \theta_{Yukawa} \in [-\pi,\pi] \sim \mathcal{O}(1)$$

  - $\bar{\theta}$ is a result of two different forces

- Neutron electric dipole moment (EDM):

$$d_N \sim 10^{-16}\,\bar{\theta}\,e\text{-cm} < 3\times 10^{-26}\,e\text{-cm} \Rightarrow$$
$$\bar{\theta} < 3\times 10^{-10}$$

- The Standard Model does not provide a reason for why $\bar{\theta}$ is so tiny – the ultimate fine-tuning problem

- In 1977, Roberto Peccei and Helen Quinn introduced a new global U(1)$_{PQ}$ symmetry that spontaneously breaks at $T = f_a \gg \Lambda_{QCD}$

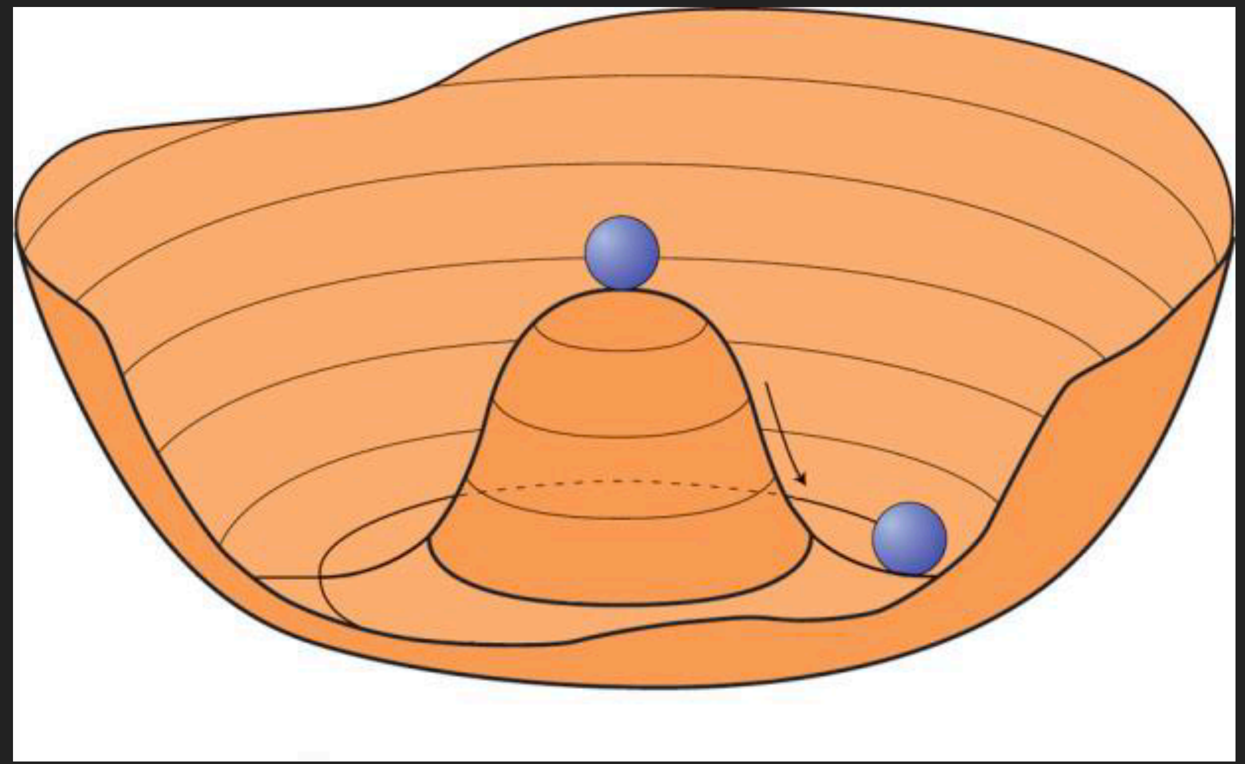

1 GeV $< T < f_a$ (PQ symmetry breaking)

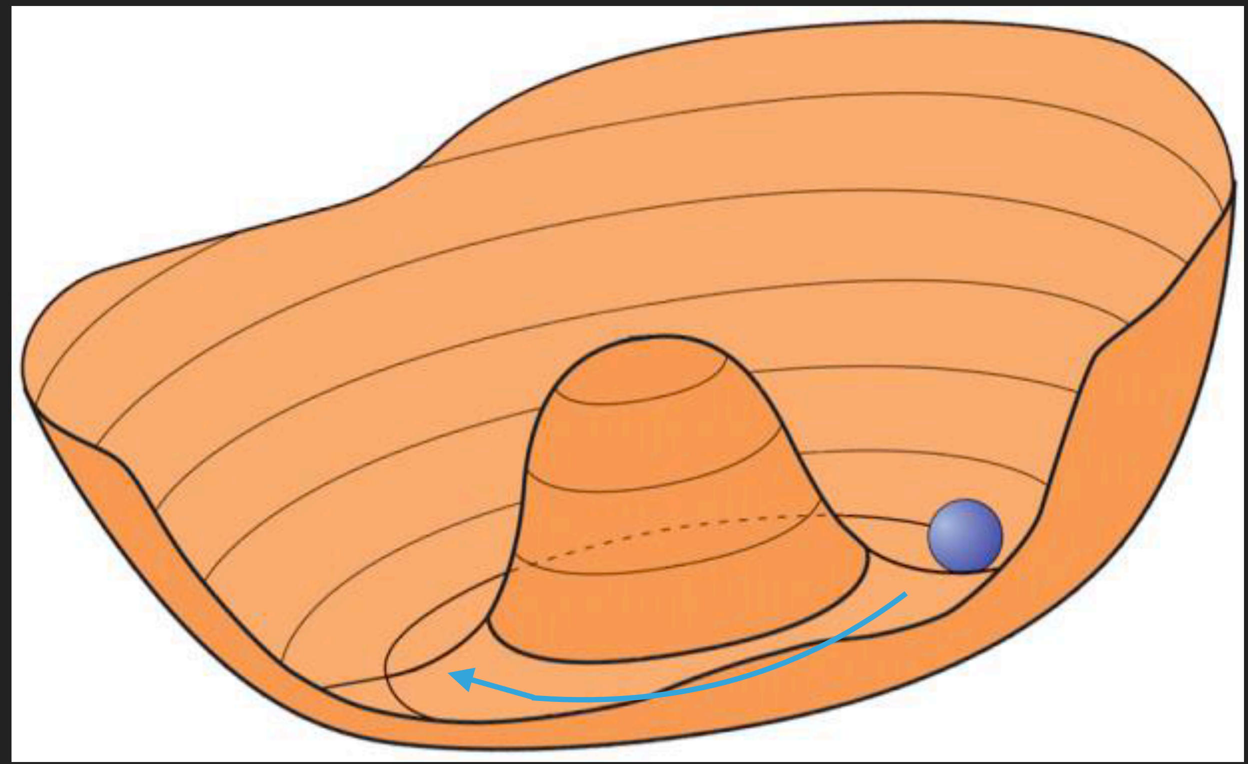

$T < 1$ GeV (QCD phase transition)

- As the universe expands, the temperature approaches the QCD phase transition $T \sim \Lambda_{QCD} \Rightarrow$ “tilt” the Mexican hat

- The axions produced by this “misalignment” mechanism are non-relativistic, and therefore can be a good CDM candidate

AXION MASS AND f_a

Scenario A: PQ symmetry breaking happens **before** inflation

$m_a < 20$ meV

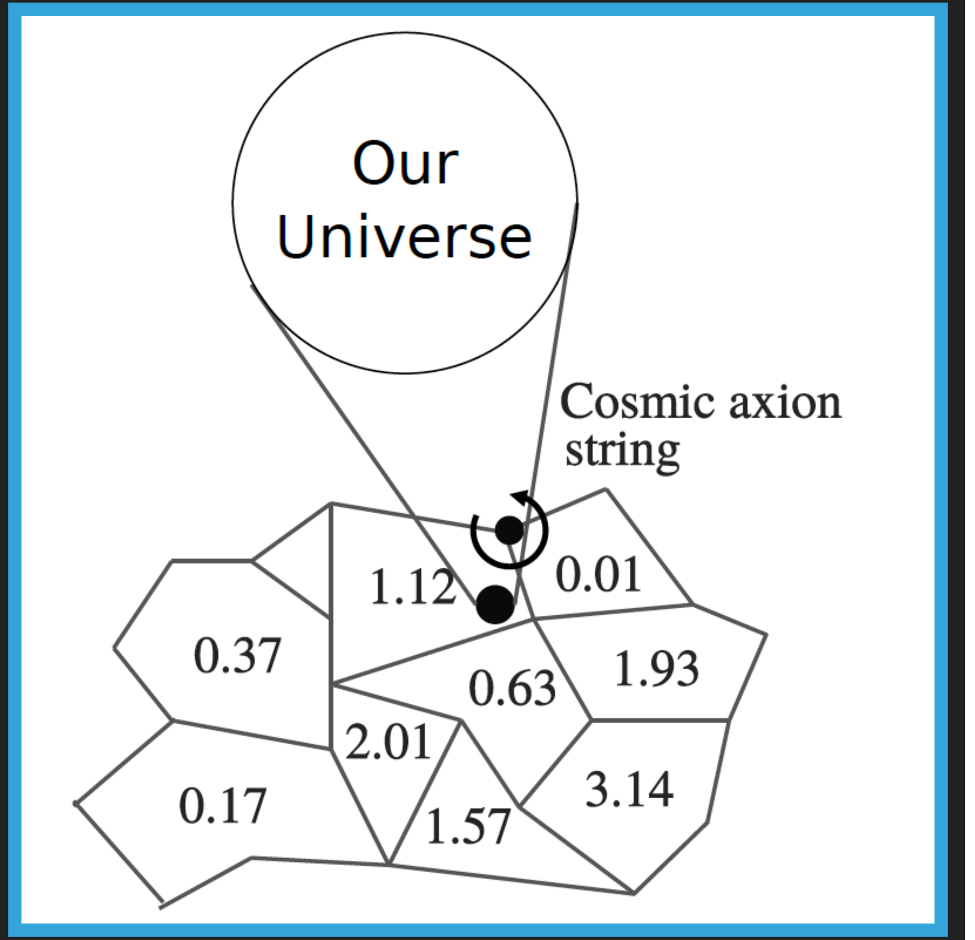

Scenario B: PQ symmetry breaking happens **after** inflation

$26\ \mu\text{eV} \lesssim m_a \lesssim 1$ meV

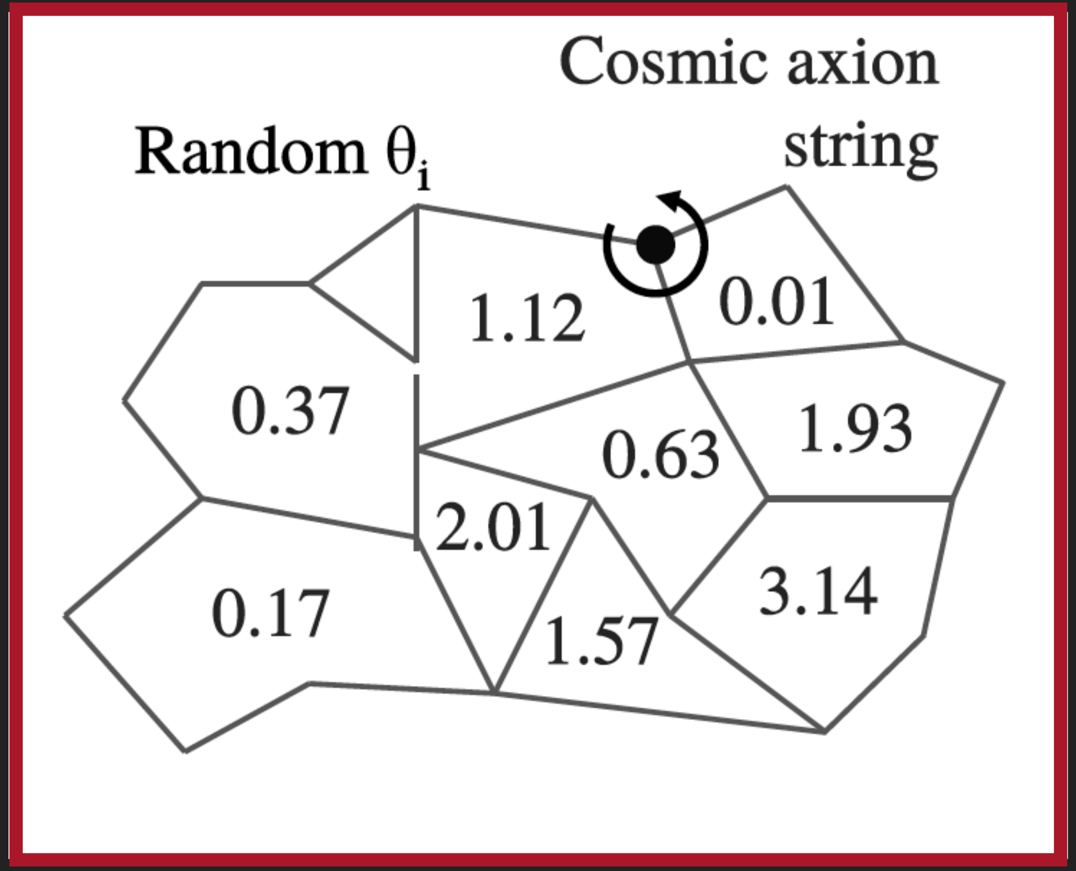

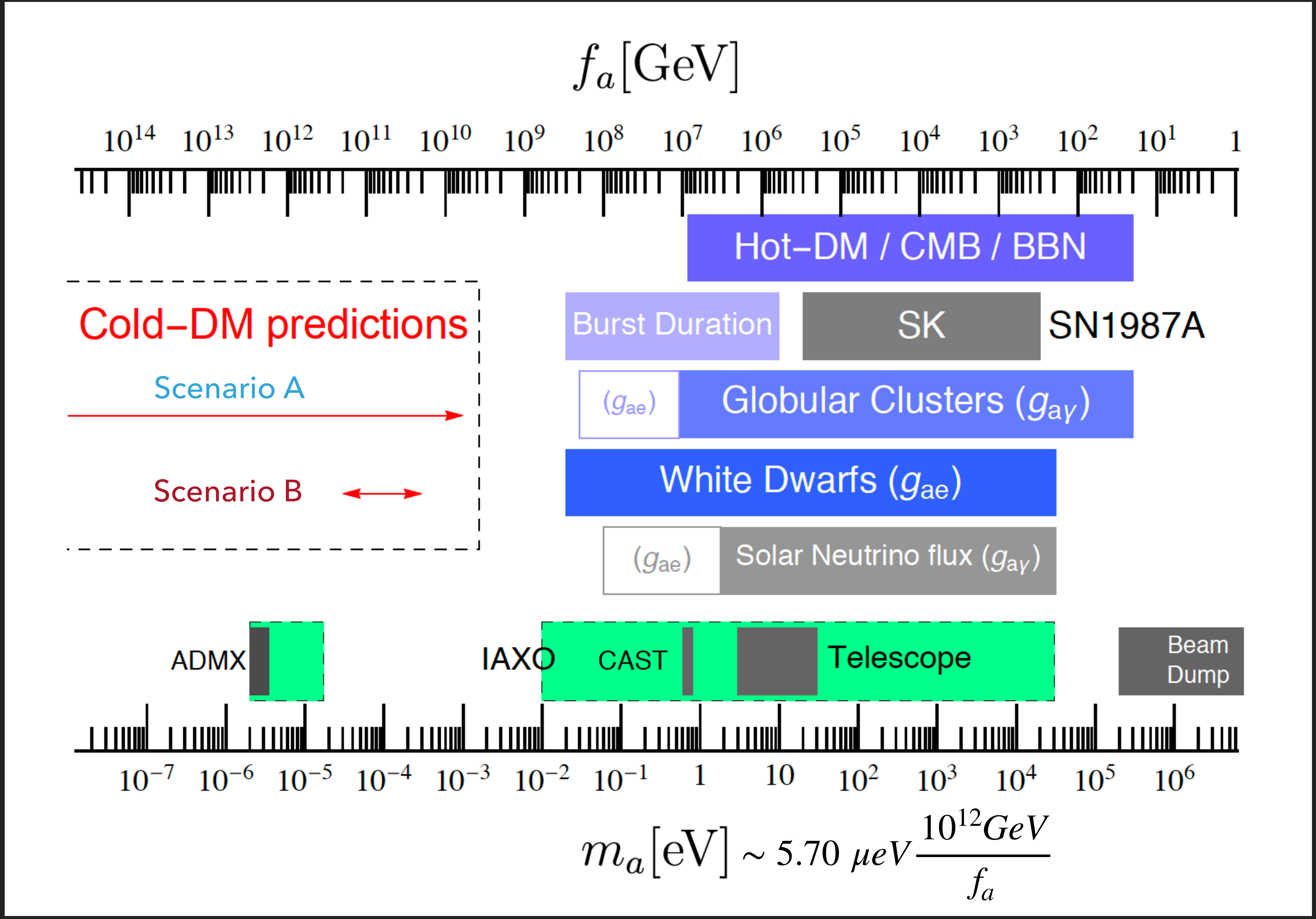

AXION DETECTION

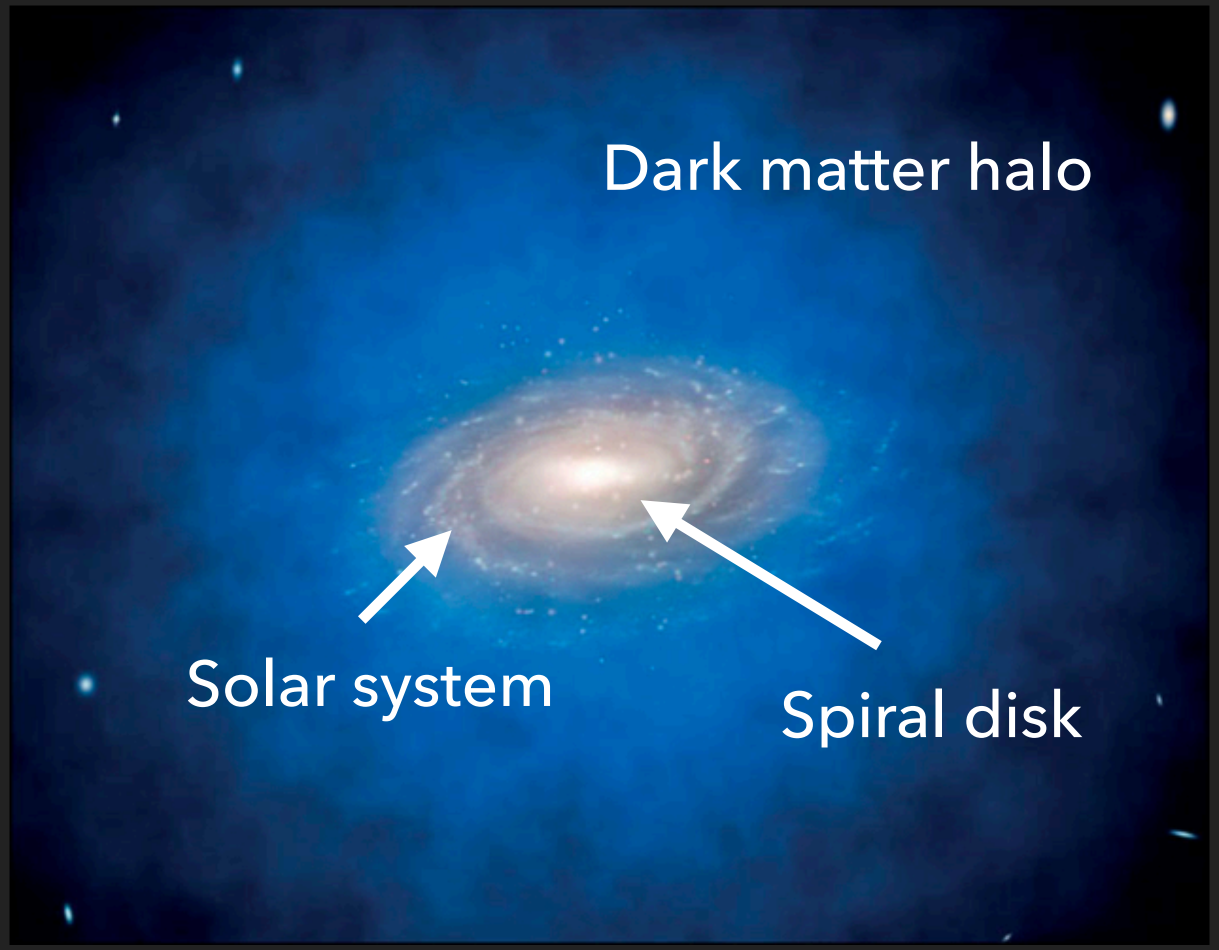

"Inverse Primakoff" process in a magnetic field

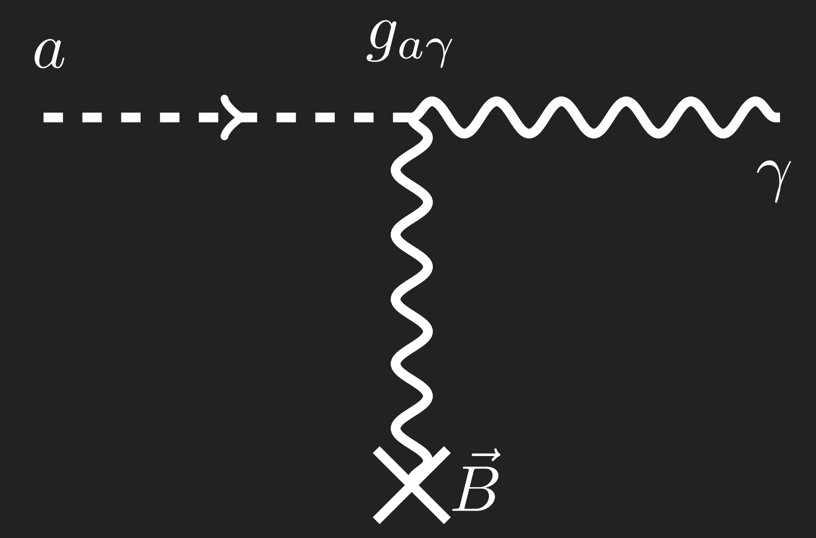

- Axion-photon coupling
  - $\mathscr{L}_{a\gamma\gamma} = -\frac{g_{a\gamma}}{4} a F_{\mu\nu}\tilde{F}^{\mu\nu} = \frac{\alpha C_{a\gamma}}{2\pi f_a} a\mathbf{E}\cdot\mathbf{B}$
  - $C_{a\gamma} = 0.36$ in the DFSZ model, $C_{a\gamma} = -0.97$ in the KSVZ model
- Local CDM axions behave like a **classical wave**: $a/f_a = \theta \approx \theta_0 \cos(m_a t)$
  - E.g. $m_a \sim 100\ \mu$eV, local galactic axion density $\rho_a = (f_a m_a)^2\theta_0^2/2 = 0.45$ GeV/cm^3
  - Axion de Broglie wavelength: $\lambda_a = \frac{2\pi}{m_a v_a} \gtrsim 10$ m $\quad (v_a \approx 10^{-3}c)$
  - Axion phase-space occupancy: $\mathcal{N}_a \sim n_a\lambda_a^3 = (\rho_a/m_a)\lambda_a^3 \sim 10^{22}$

Macroscopic axion-Maxwell equation under external B-field

$$\nabla\cdot\mathbf{D} = \rho_f - g_{a\gamma}\mathbf{B}_e\cdot\nabla a$$
$$\nabla\times\mathbf{H} - \partial_t\mathbf{D} = \mathbf{J}_f - g_{a\gamma}(\mathbf{E}\times\nabla a - \mathbf{B}_e\partial_t a)$$
$$\nabla\times\mathbf{E} + \partial_t\mathbf{B} = 0$$
$$\nabla\cdot\mathbf{B} = 0$$
$$\partial_t^2 a - \nabla^2 a + m_a^2 a = g_{a\gamma}\mathbf{E}\cdot\mathbf{B}_e$$

AXION DETECTION

- Axion-photon coupling
  - $\mathscr{L}_{a\gamma\gamma} = -\frac{g_{a\gamma}}{4} a F_{\mu\nu} \tilde{F}^{\mu\nu} = \frac{\alpha C_{a\gamma}}{2\pi f_a} a \mathbf{E} \cdot \mathbf{B}$
  - $C_{a\gamma} = 0.36$ in the DFSZ model, $C_{a\gamma} = -0.97$ in the KSVZ model

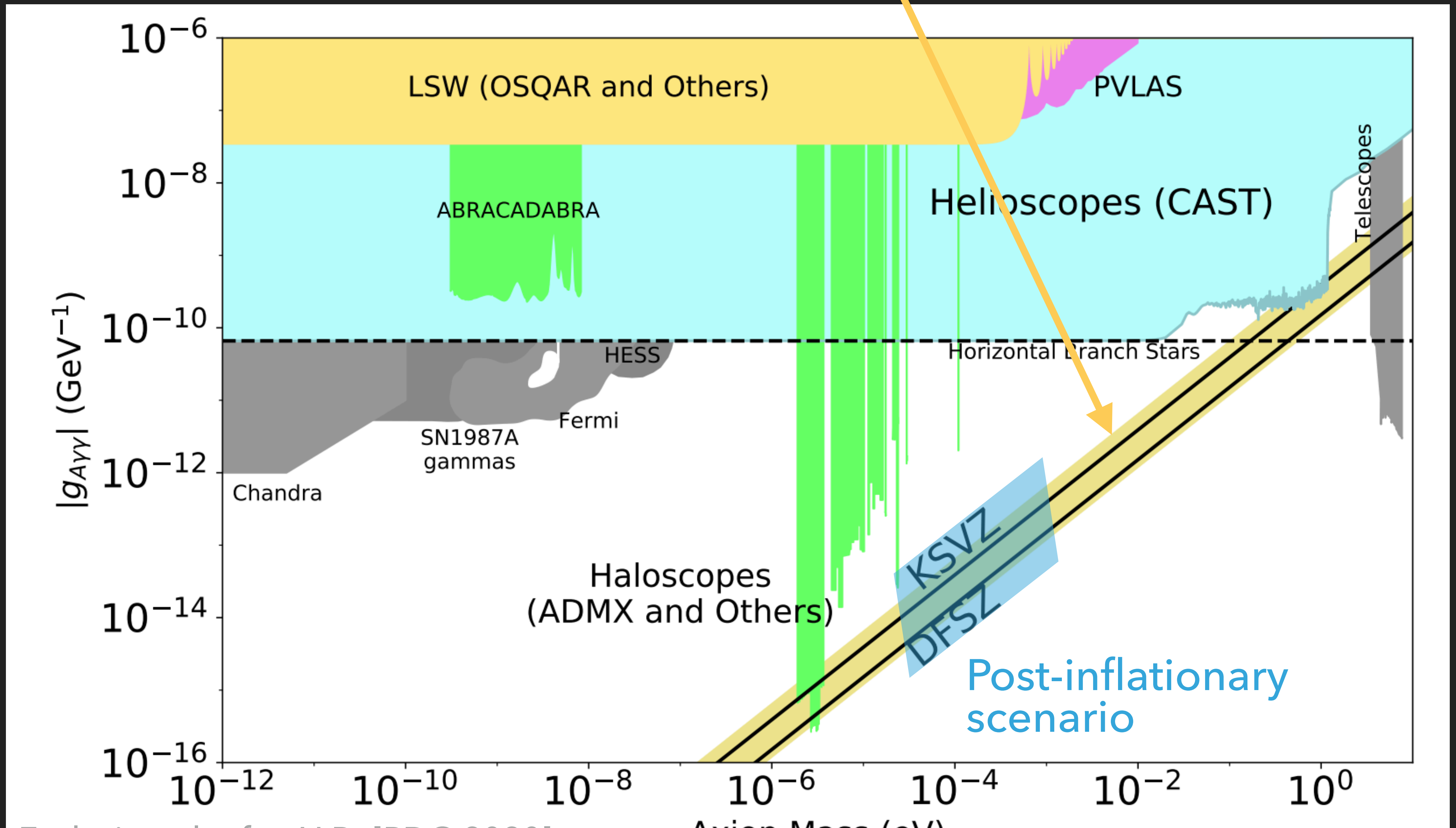

Exclusion plot for ALPs [PDG 2020]

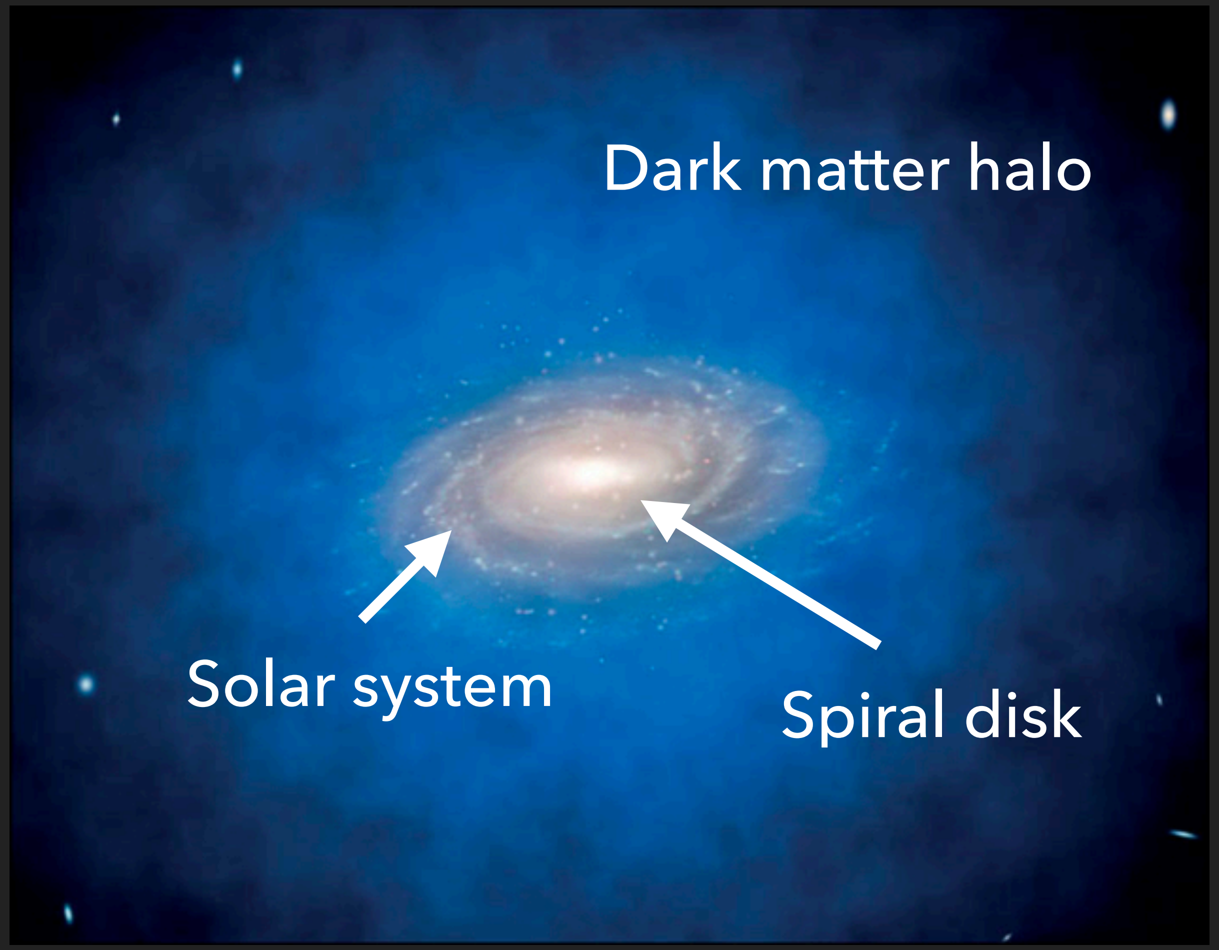

"Inverse Primakoff" process in a magnetic field

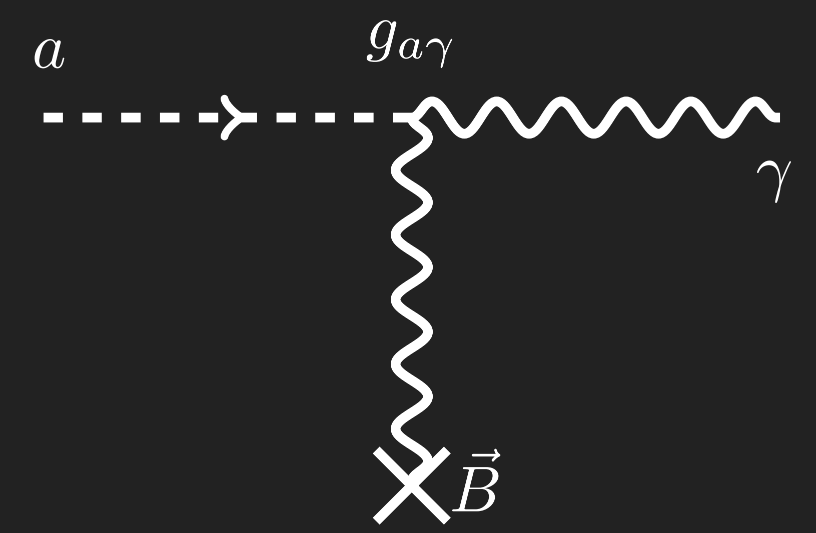

Macroscopic axion-Maxwell equation under external B-field

$$\nabla \cdot \mathbf{D} = \rho_f - g_{a\gamma} \mathbf{B}_e \cdot \nabla a$$

$$\nabla \times \mathbf{H} - \partial_t \mathbf{D} = \mathbf{J}_f - g_{a\gamma} (\mathbf{E} \times \nabla a - \mathbf{B}_e \partial_t a)$$

$$\nabla \times \mathbf{E} + \partial_t \mathbf{B} = 0$$

$$\nabla \cdot \mathbf{B} = 0$$

$$\partial_t^2 a - \nabla^2 a + m_a^2 a = g_{a\gamma} \mathbf{E} \cdot \mathbf{B}_e$$

AXION HALOSCOPE

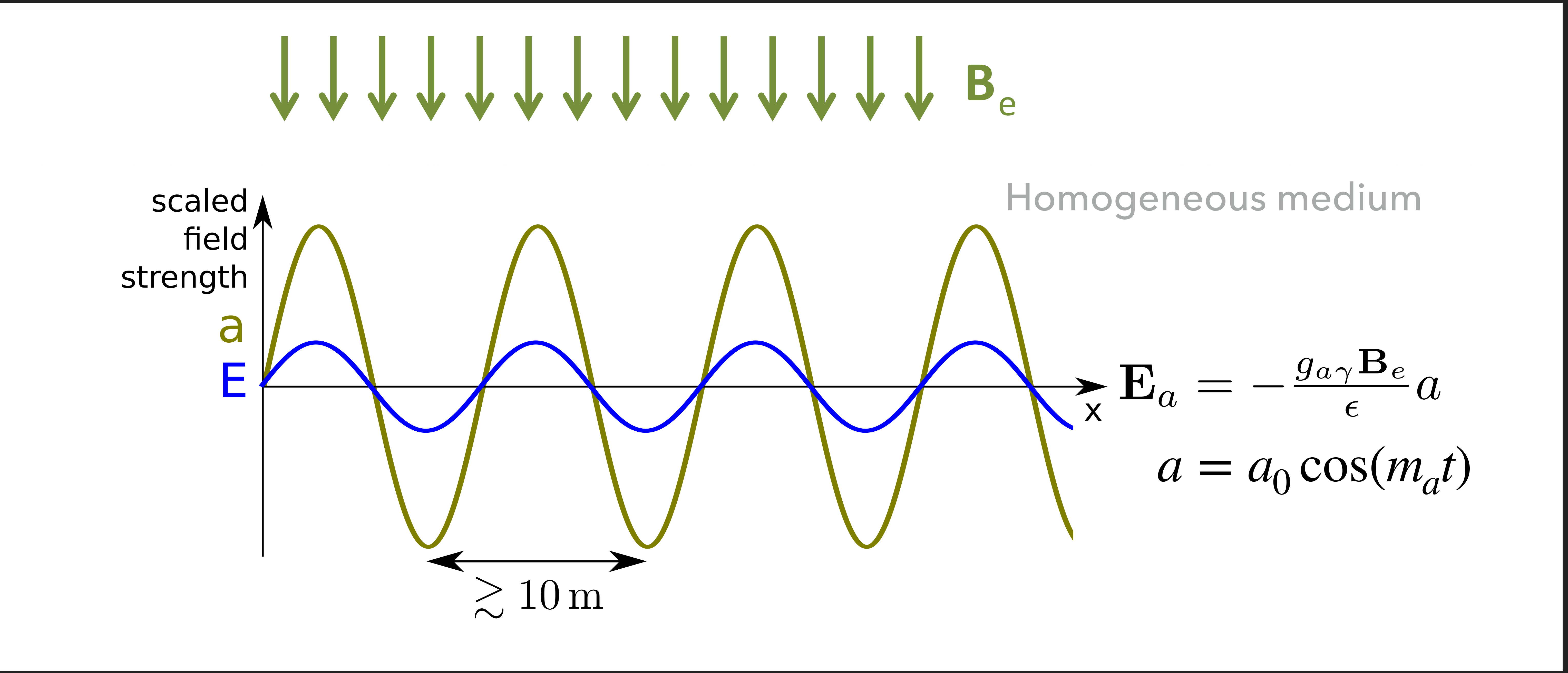

$$\nabla^2 \mathbf{E} - \partial_t^2 \mathbf{E} = -\frac{g_{a\gamma}\mathbf{B}_e \partial_t^2 a}{\epsilon}$$

$$\Uparrow$$

Leading term

$$\nabla \cdot \mathbf{D} = \rho_f - g_{a\gamma}\cancel{\mathbf{B}_e \cdot} \nabla a$$

$$\nabla \times \mathbf{H} - \partial_t \mathbf{D} = \mathbf{J}_f - g_{a\gamma}(\cancel{\mathbf{E} \times \nabla a} - \mathbf{B}_e \partial_t a)$$

$$\nabla \times \mathbf{E} + \partial_t \mathbf{B} = 0$$

$$\nabla \cdot \mathbf{B} = 0$$

$$\partial_t^2 a - \nabla^2 a + m_a^2 a = g_{a\gamma}\mathbf{E} \cdot \mathbf{B}_e$$

- Axion induced electric field:

Local axion DM density

$$|\mathbf{E}_a| = \left| -\frac{g_{a\gamma}\mathbf{B}_e}{\epsilon} a \right| = 1.3 \times 10^{-12}\,\mathrm{Vm}^{-1} \times \left(\frac{B_e}{10\,\mathrm{T}}\right) \left(\frac{\rho_a}{300\,\mathrm{MeV/cm}^3}\right)^{1/2} \frac{C_{a\gamma}}{\epsilon}$$

Dielectric constant

CAVITY HALOSCOPE (1)

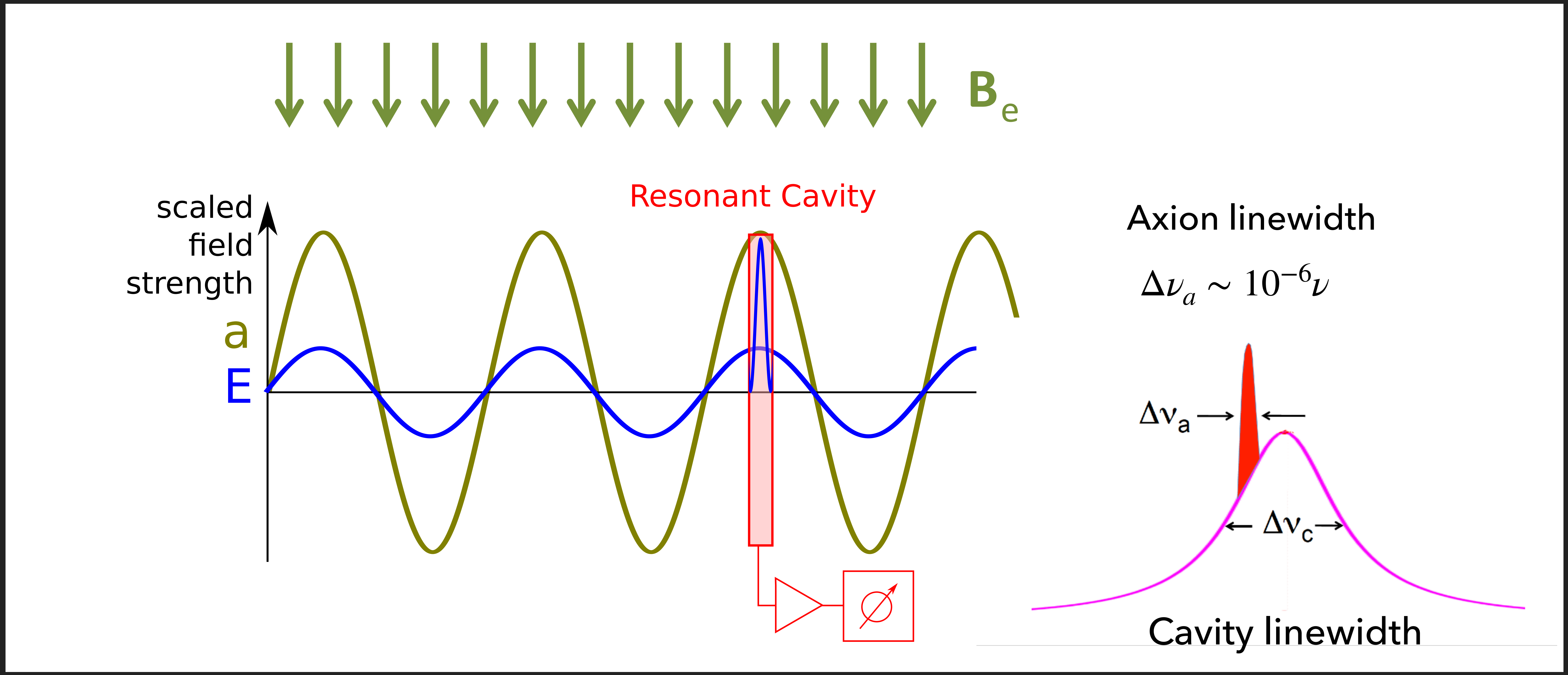

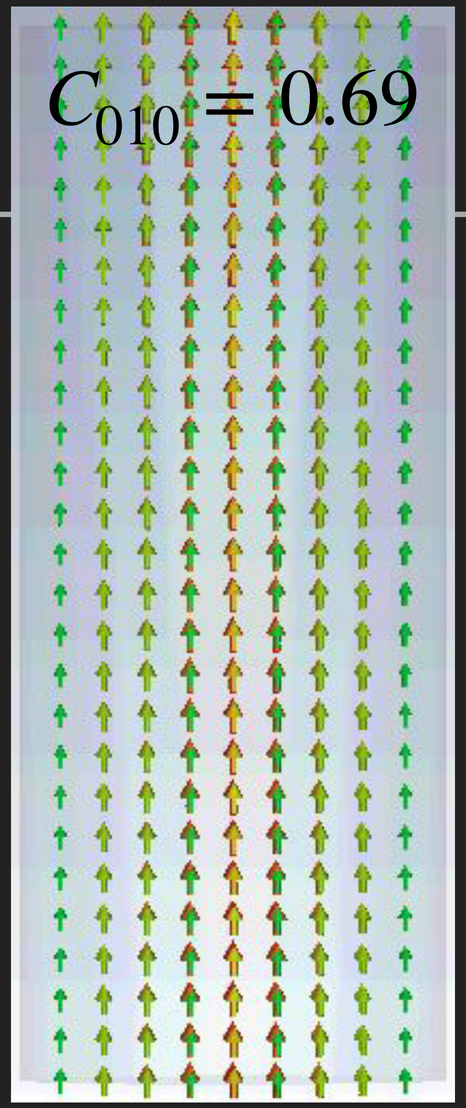

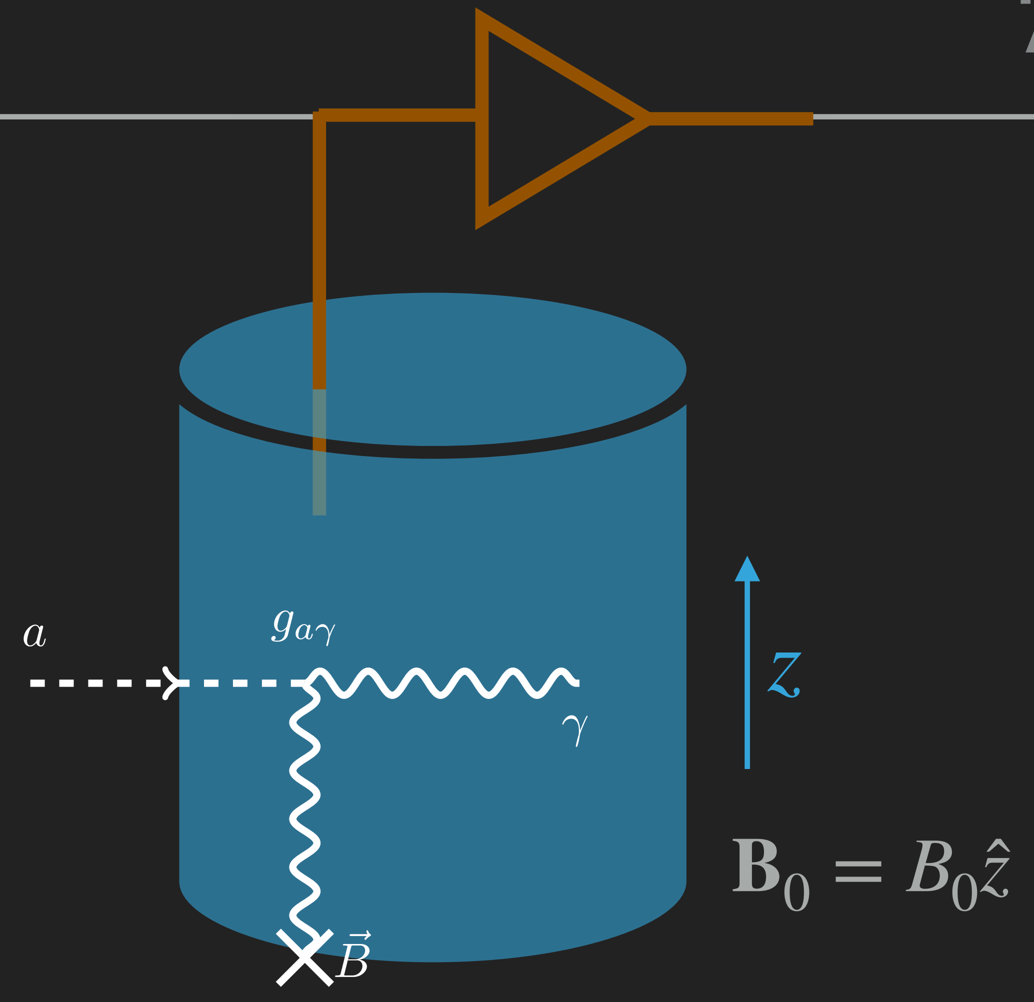

- Axion signal can be enhanced to a level detectable by a low noise amplifier

$$P_{sig} \sim 1.9 \times 10^{-22}\,\mathrm{W} \left(\frac{V}{136L}\right)\left(\frac{B_e}{6.8T}\right)^2\left(\frac{C}{0.4}\right)\left(\frac{C_{a\gamma\gamma}}{0.97}\right)^2\left(\frac{\rho_a}{0.45\ \mathrm{GeV\ cm^{-3}}}\right)\left(\frac{f}{650\ \mathrm{MHz}}\right)\left(\frac{Q}{50{,}000}\right)$$

Cavity volume

Cavity form factor

Cavity Quality factor

CAVITY HALOSCOPE (2)

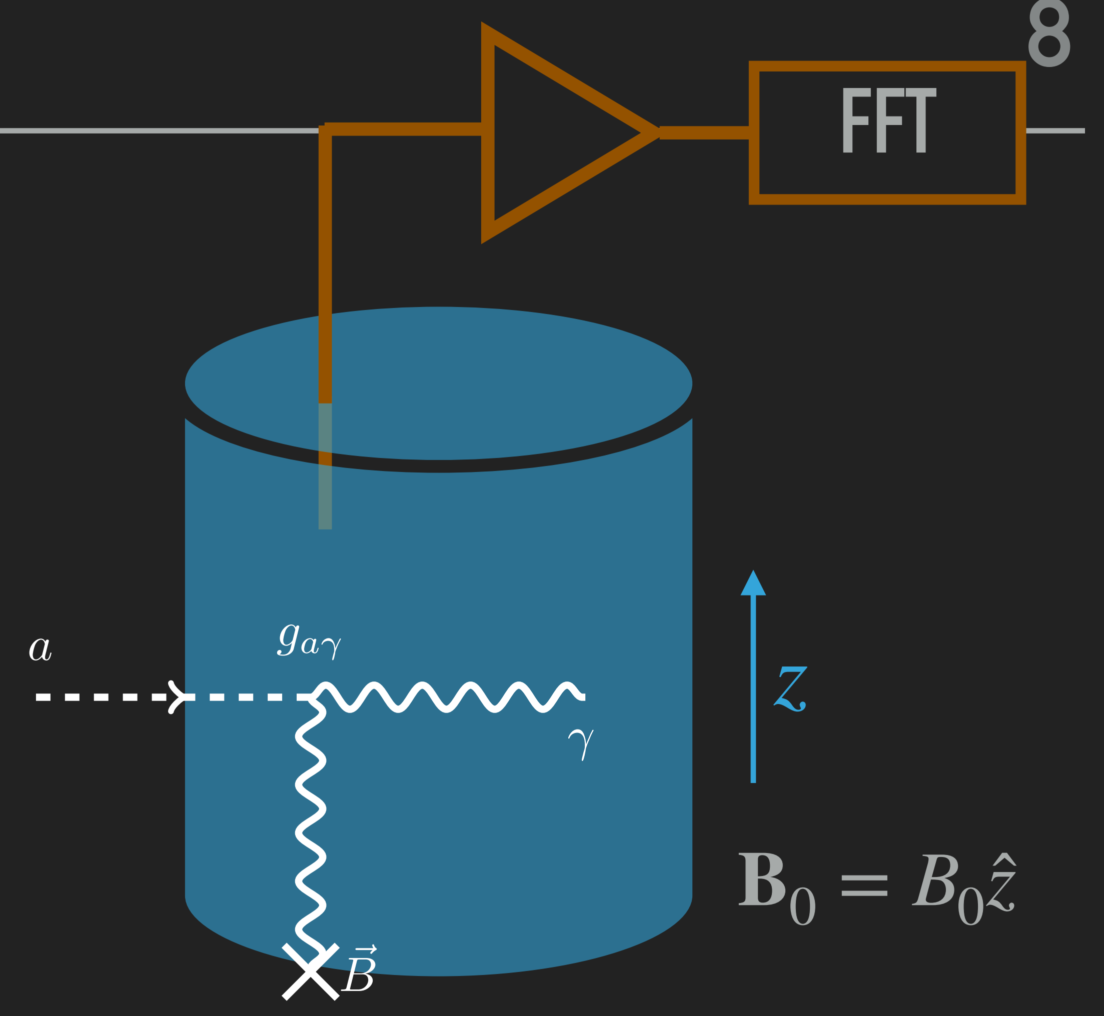

- The "signal" that the receiver measures is mostly noise
  - Cavity wall resistivity ⇒ Johnson noise, or thermal noise
  - The receiver itself has noise
  - Total power within bandwidth $\Delta\nu$: $P_N = k_B T_{sys} \Delta\nu$, where T_{sys} is the system noise temperature. $P_N \gg P_{sig}$
- Dicke radiometer equation: $SNR = \dfrac{P_{sig}}{\delta P_N} = \dfrac{P_{sig}}{k_B T_{sys}}\sqrt{\dfrac{\tau}{\Delta\nu_a}}$

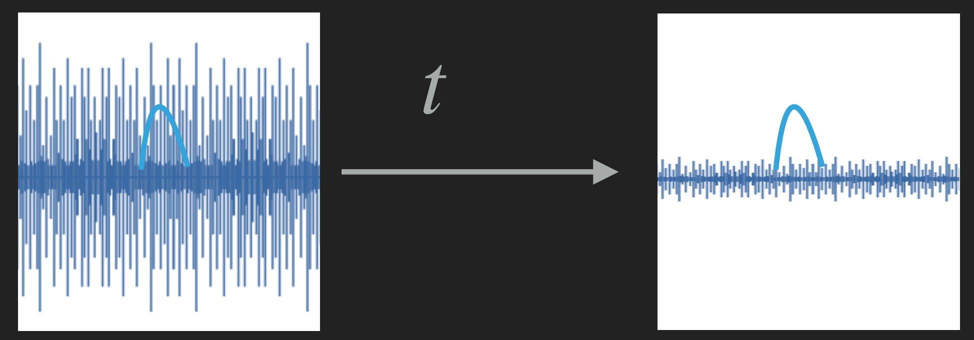

Power spectral density

$$P_{sig} \sim 1.9 \times 10^{-22}\,\mathrm{W}\left(\frac{V}{136L}\right)\left(\frac{B_e}{6.8T}\right)^2\left(\frac{C}{0.4}\right)\left(\frac{C_{a\gamma\gamma}}{0.97}\right)^2\left(\frac{\rho_a}{0.45\ \mathrm{GeV\ cm}^{-3}}\right)\left(\frac{f}{650\ \mathrm{MHz}}\right)\left(\frac{Q}{50{,}000}\right)$$

Cavity volume

Cavity form factor

Cavity Quality factor

HIGH FREQUENCY CHALLENGES WITH CAVITY HALOSCOPES

- Cavity haloscope signal power

ADMX: $$P_{sig} \approx 1.9 \times 10^{-22}\,\mathrm{W} \left(\frac{V}{136\ L}\right)\left(\frac{C}{0.4}\right)\left(\frac{B_e}{6.8T}\right)^2\left(\frac{C_{a\gamma}}{0.97}\right)^2\left(\frac{\rho_a}{0.45\ \mathrm{GeV\ cm^{-3}}}\right)\left(\frac{f}{650\ \mathrm{MHz}}\right)\left(\frac{Q}{50{,}000}\right)$$

HAYSTAC: $$P_{sig} \approx 5 \times 10^{-24}\,\mathrm{W} \left(\frac{V}{1.5\ L}\right)\left(\frac{C}{0.5}\right)\left(\frac{B_e}{9T}\right)^2\left(\frac{C_{a\gamma}}{0.97}\right)^2\left(\frac{\rho_a}{0.45\ \mathrm{GeV\ cm^{-3}}}\right)\left(\frac{f}{5\ \mathrm{GHz}}\right)\left(\frac{Q}{10{,}000}\right)$$

- $V \cdot C$ is scaled by Compton wavelength
- Quality factor Q decreases for higher frequencies due to the skin effect
- Increasing B_e is very costly
- Lower bound on T_{sys} by quantum physics
- New detector concept is needed at higher frequencies (higher axion mass)

DIELECTRIC HALOSCOPE

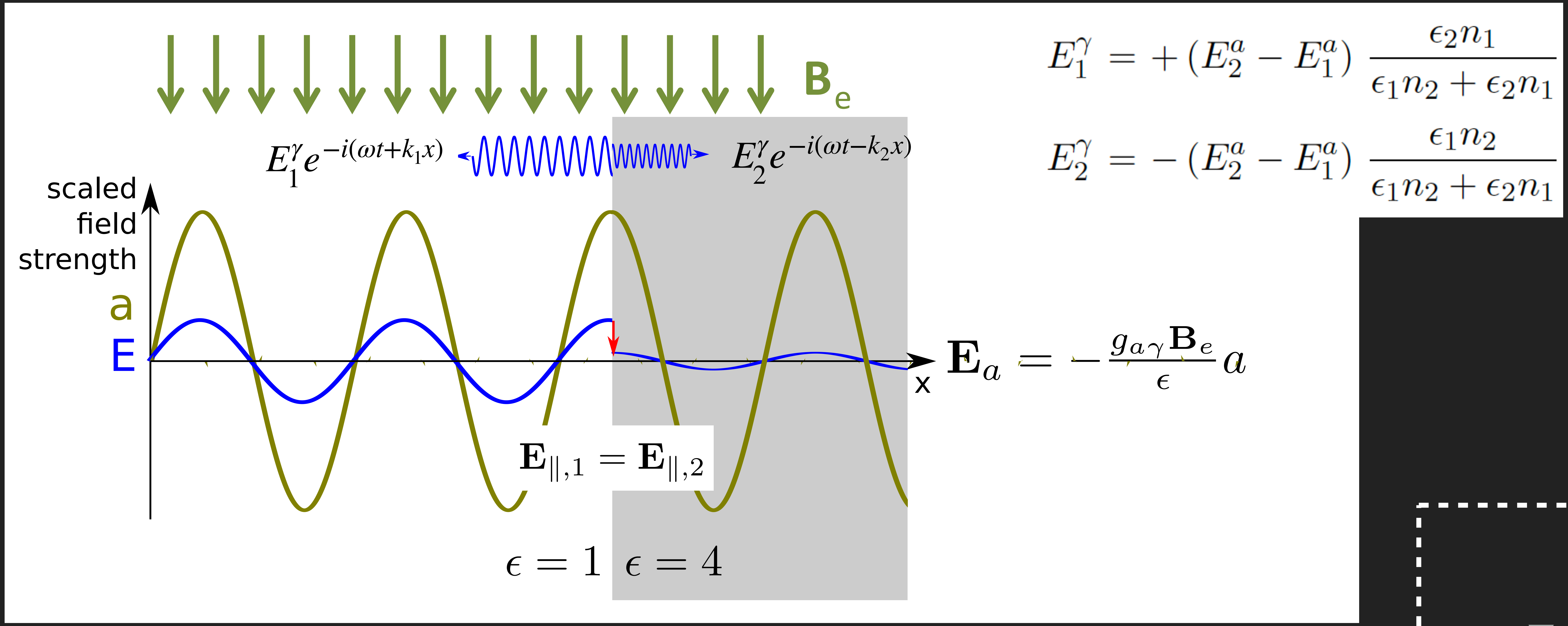

- $E_{//}$ is continuous at dielectric boundaries ⇒ EM radiation

Leading term

$$\nabla \cdot \mathbf{D} = \rho_f - g_{a\gamma} \cancel{\mathbf{B}_e \cdot \nabla a}$$

$$\nabla \times \mathbf{H} - \partial_t \mathbf{D} = \mathbf{J}_f - g_{a\gamma}(\cancel{\mathbf{E} \times \nabla a} - \mathbf{B}_e \partial_t a)$$

$$\nabla \times \mathbf{E} + \partial_t \mathbf{B} = 0$$

$$\nabla \cdot \mathbf{B} = 0$$

$$\partial_t^2 a - \nabla^2 a + m_a^2 a = g_{a\gamma} \mathbf{E} \cdot \mathbf{B}_e$$

- Power emitted at a vacuum-to-perfect-conductor interface:

$$\frac{P^\gamma_{sig}}{A} = 2.2 \times 10^{-27} \frac{\mathrm{W}}{\mathrm{m}^2} \left(\frac{B_e}{10\,\mathrm{T}}\right)^2 C_{a\gamma}^2$$

MAgnetized Disc and Mirror Axion eXperiment (MADMAX)

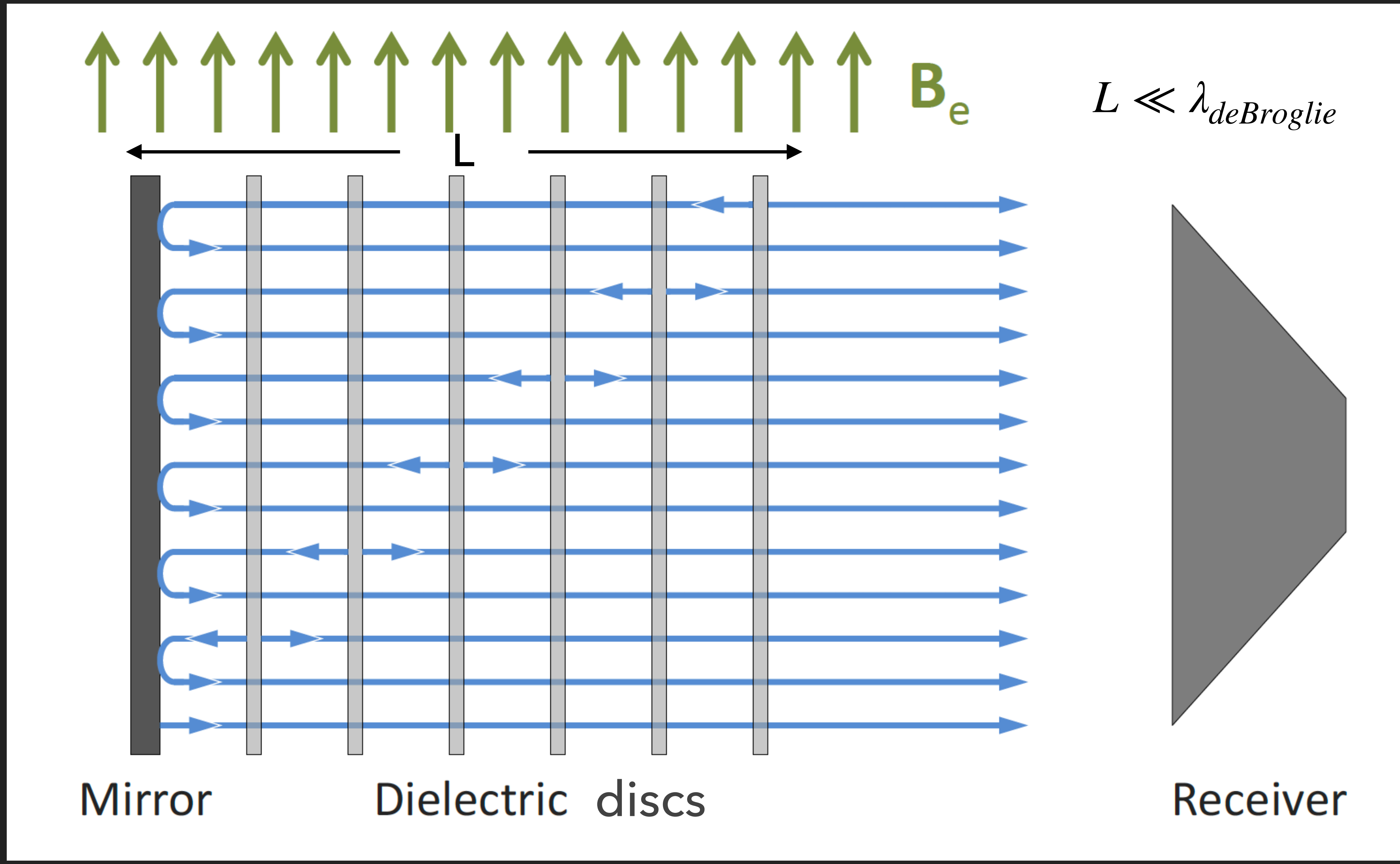

Cryogenic environment to lower the system noise temperature

- Two effects contributing to the power enhancement at selected frequencies
  - Coherent emission from each interface
  - Resonance effects within the the mirror+disc system

$$\frac{P^{\gamma}_{sig}}{A} = 2.2 \times 10^{-27} \frac{\mathrm{W}}{\mathrm{m}^2} \left(\frac{B_e}{10\,\mathrm{T}}\right)^2 C^2_{a\gamma} \cdot \beta^2 \longrightarrow \text{Boost factor } \beta^2 \geq 10^4 \text{ achievable}$$

~m²

PROPERTIES OF THE "BOOST FACTOR"

- Area law: $\int \left|\beta(\nu)\right|^2 \mathrm{d}\nu \propto N$
  - Options for broadband and narrowband scans

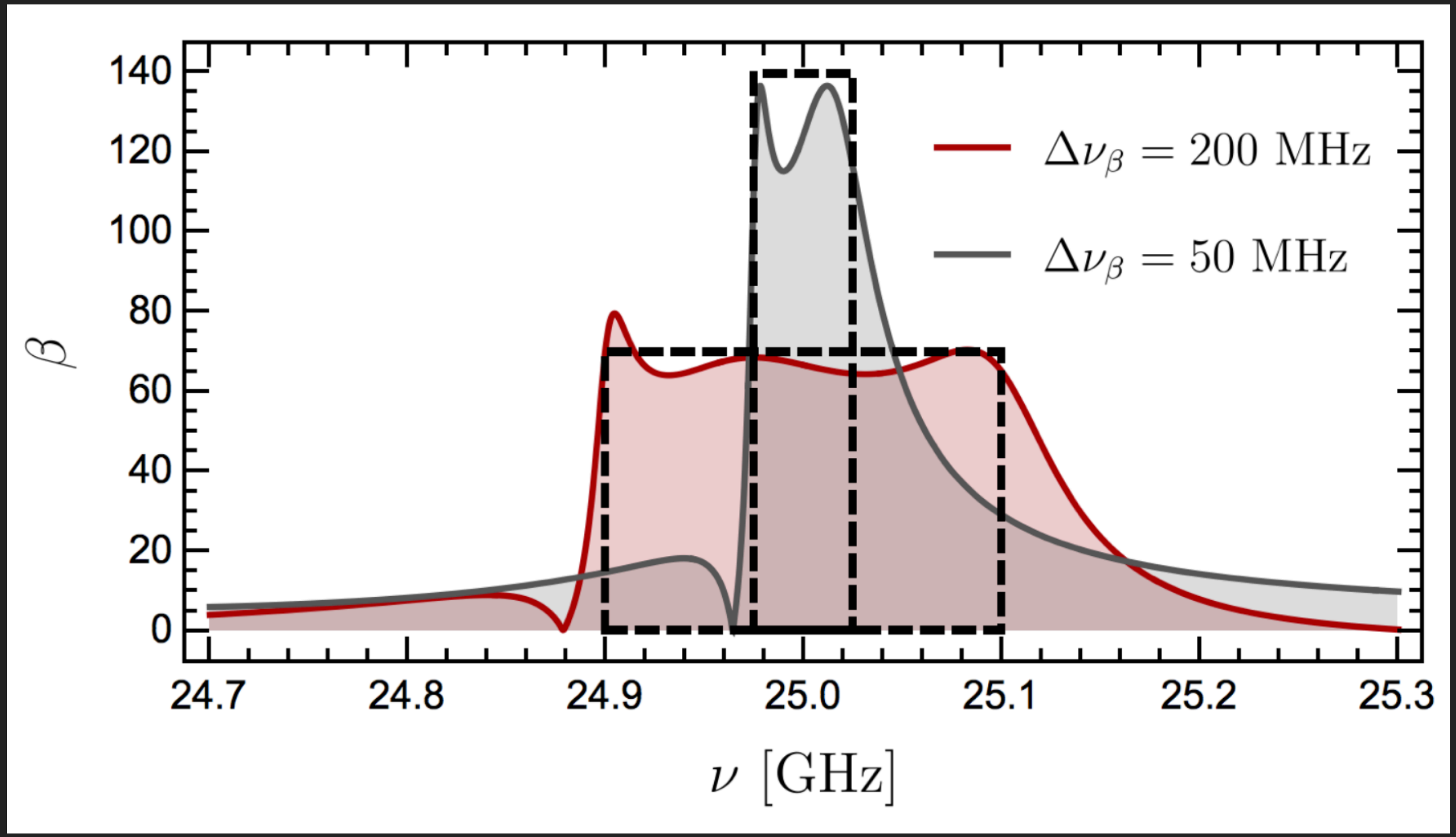

- Frequency tuning of the boost factor possible

Disc positions randomly varied by $\sigma = 15\ \mu$m

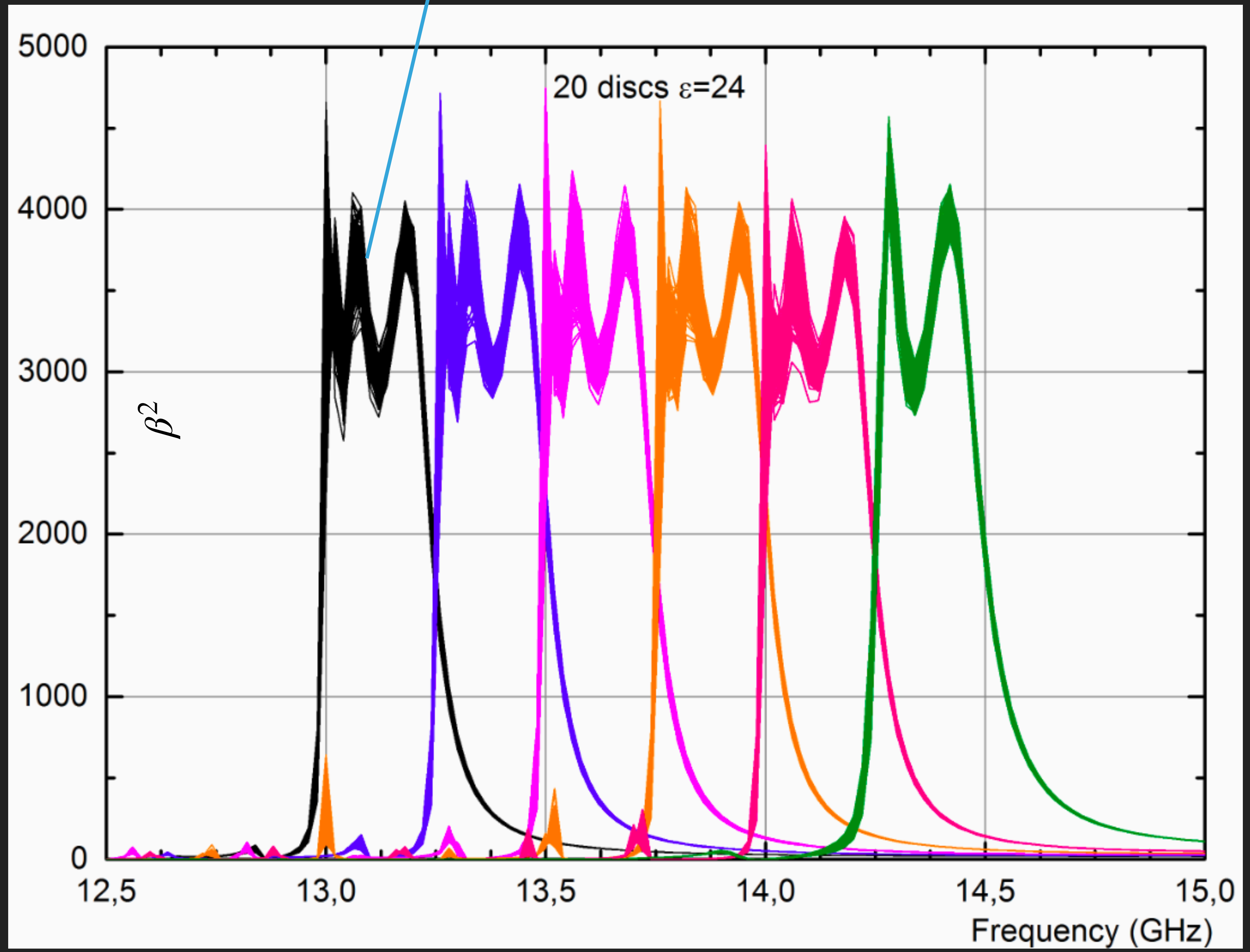

Frequency can be tuned by changing the disc positions

MADMAX TARGET DESIGN

Signal power: $P^{\gamma}_{sig} = 2.2 \times 10^{-27} W \left(\frac{A}{1\ \mathrm{m}^2}\right) \left(\frac{B_0}{10\ \mathrm{T}}\right)^2 C^2_{a\gamma} \cdot \beta^2$, where $\beta^2 \sim 10^5$

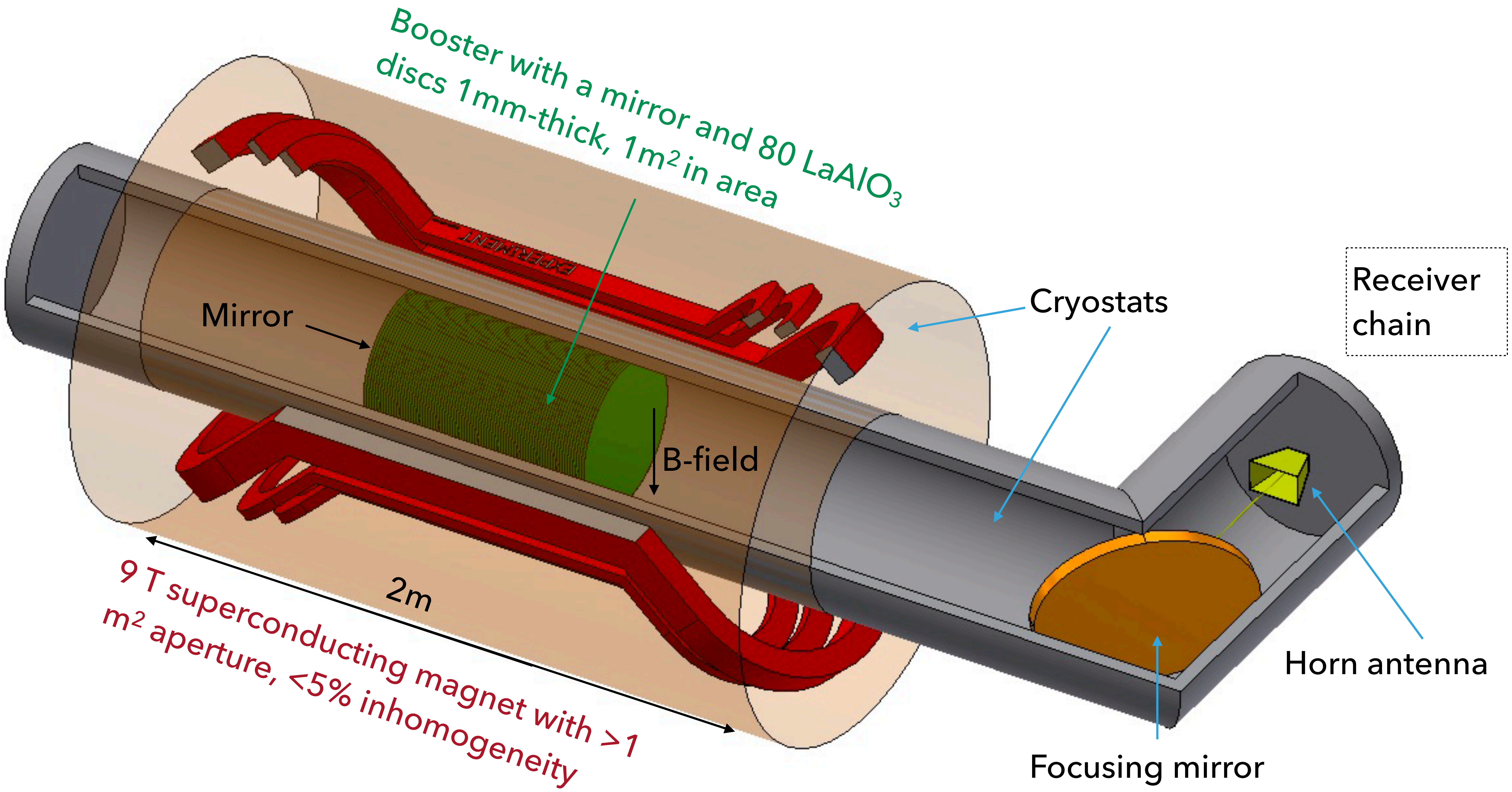

Designed to search for QCD axions that make up the galactic dark matter halo

EXPERIMENTAL CHALLENGES

1. The biggest challenge for MADMAX is estimating the boost factor
   - The boost factor is not a measurable quantity
   - The strategy is to estimate the boost factor using a model, which is constrained by measurable quantities such as the reflectivity and noise
   - Measurement based frequency tuning to mitigate the limitations from modeling
   - **work in progress!**
2. 3D effects can have significant impact on the boost factor
3. RF receiver chain to detect a signal of $\lesssim 10^{-22}$ W at 4 K
4. Engineering challenges
   - E.g. high field (~9T), large bore (~m^2) magnet

THE PROOF-OF-PRINCIPLE SETUP @ MPP

Corrugated horn antenna

arXiv:2001.04363

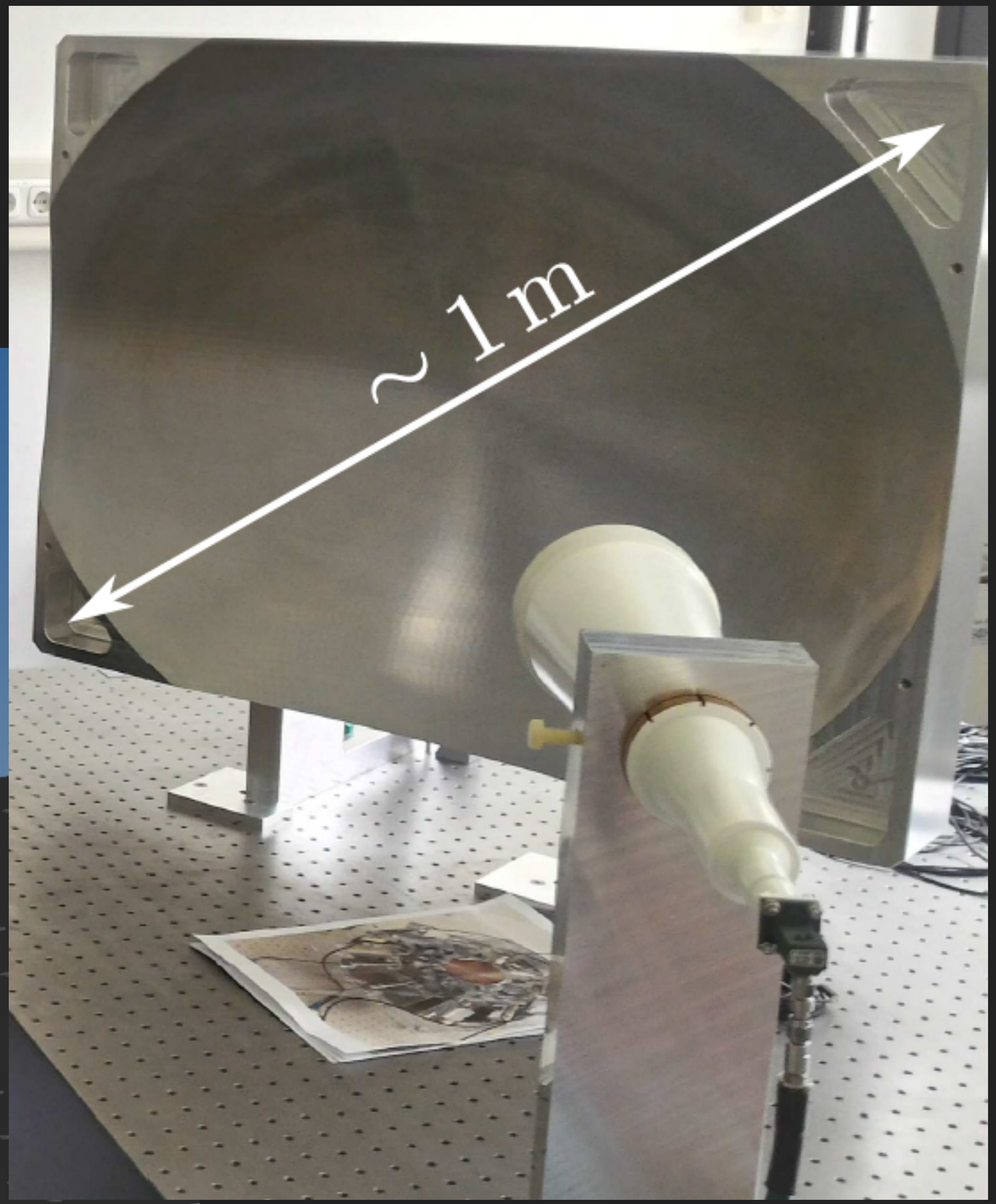

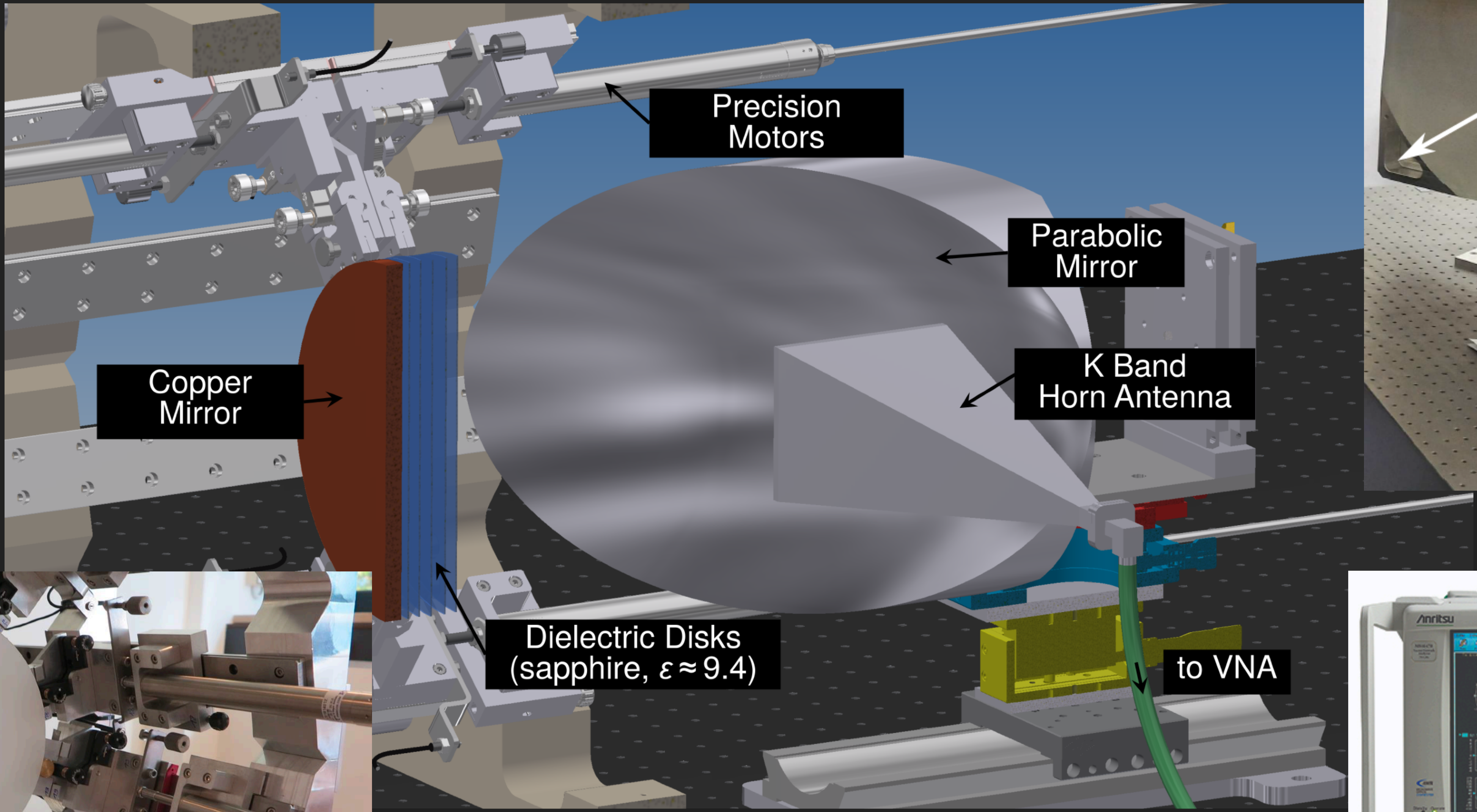

Up to 20 Ø 20cm sapphire discs

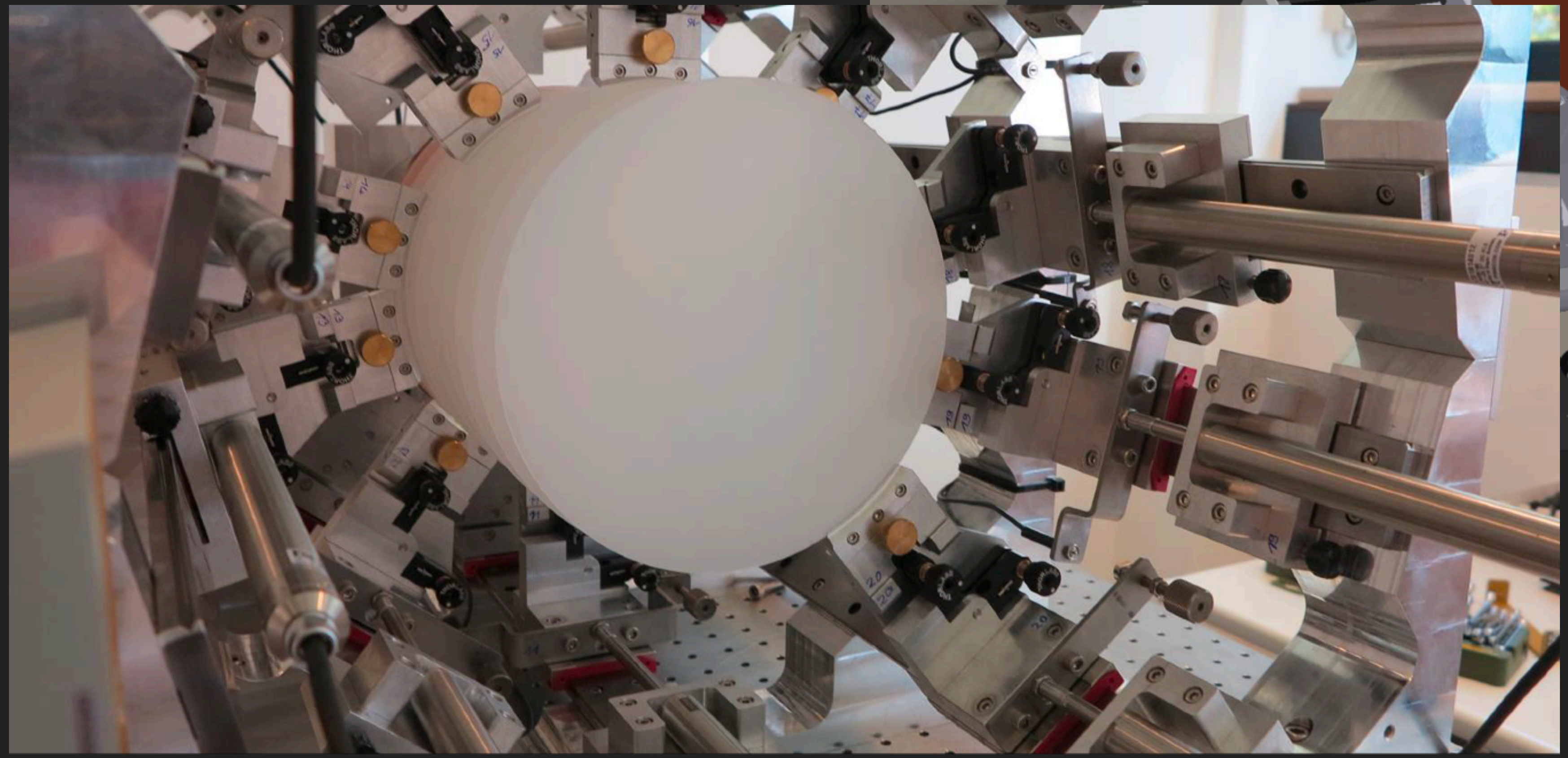

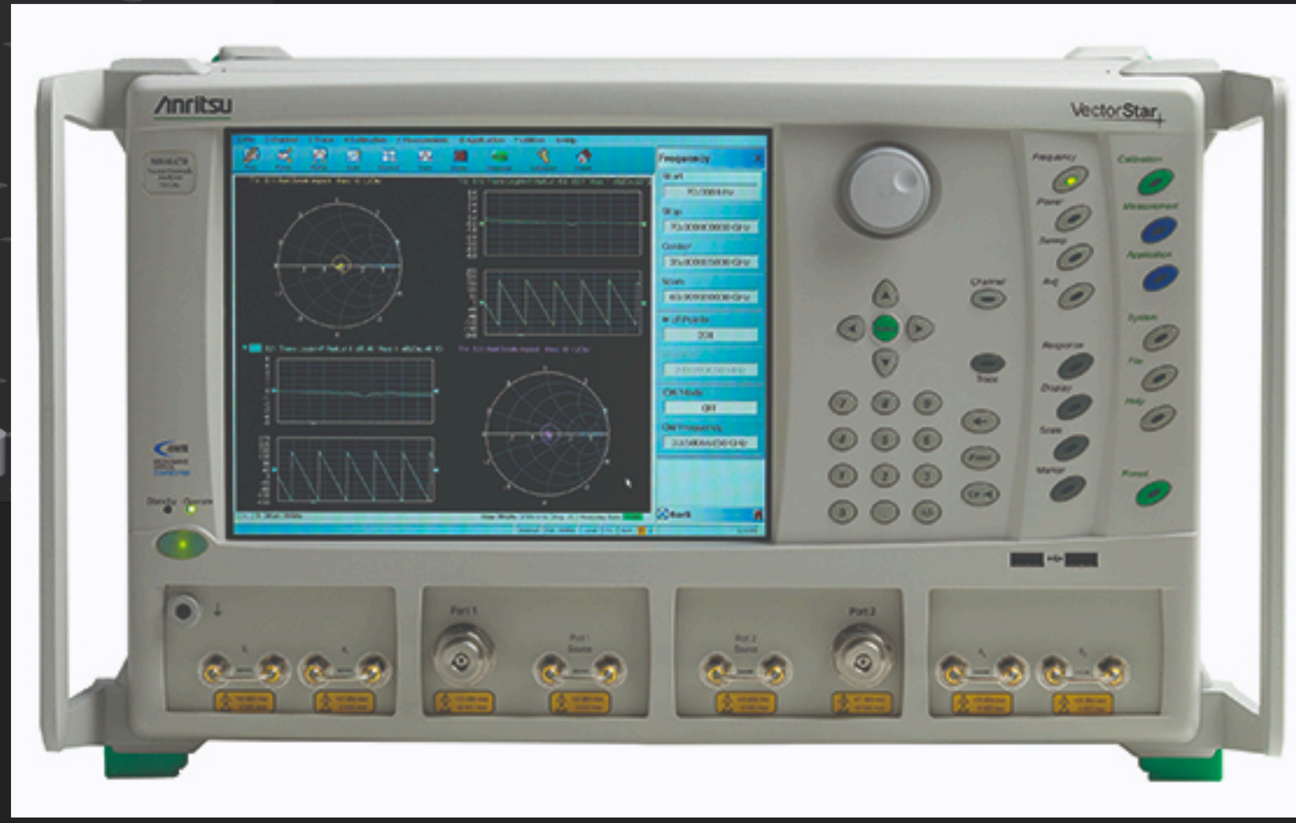

Vector Network Analyzer

FREQUENCY TUNING WITH THE POP SETUP (1)

An example of the group delay measurement with 4 discs in the POP setup

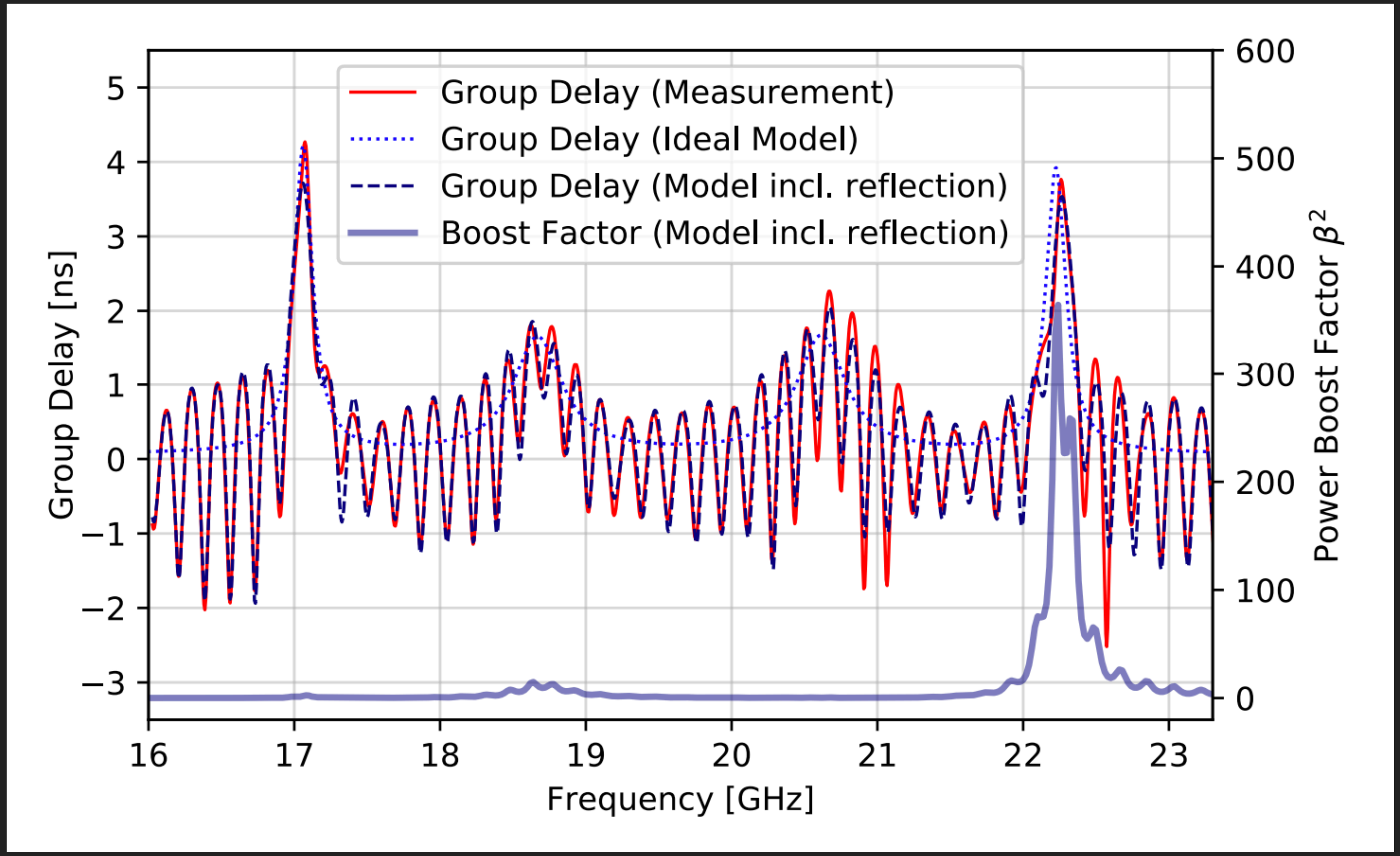

* boost factor calculated using 1D model

- Frequency tuning procedure:
  - Calculate group delay with the same disc configuration that yields the desired boost factor
  - Move the discs in the POP setup iteratively until the measurement matches the calculated group delay
- Advantages of measurement guided tuning
  - Absolutely disc positions unknown
  - Discrepancies between simulation and measurement
    - Unknown parameters such as disc ϵ, surface flatness, etc.
  - The procedure can help mitigate the impact of inaccuracies that introduce phase errors

FREQUENCY TUNING WITH THE POP SETUP (2)

An example of the group delay measurement with 4 discs in the POP setup

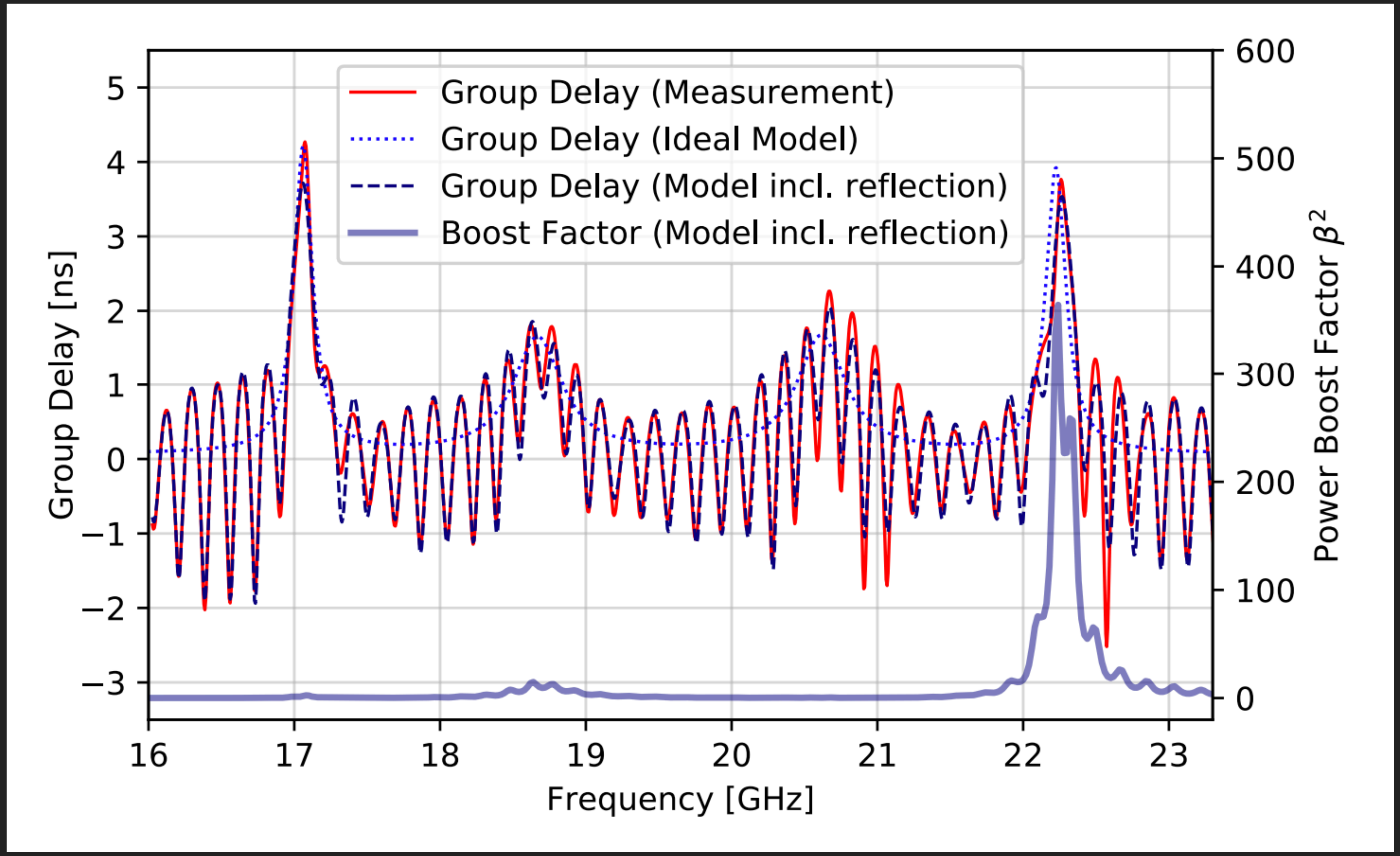

* boost factor calculated using 1D model

2 disc tuning result →

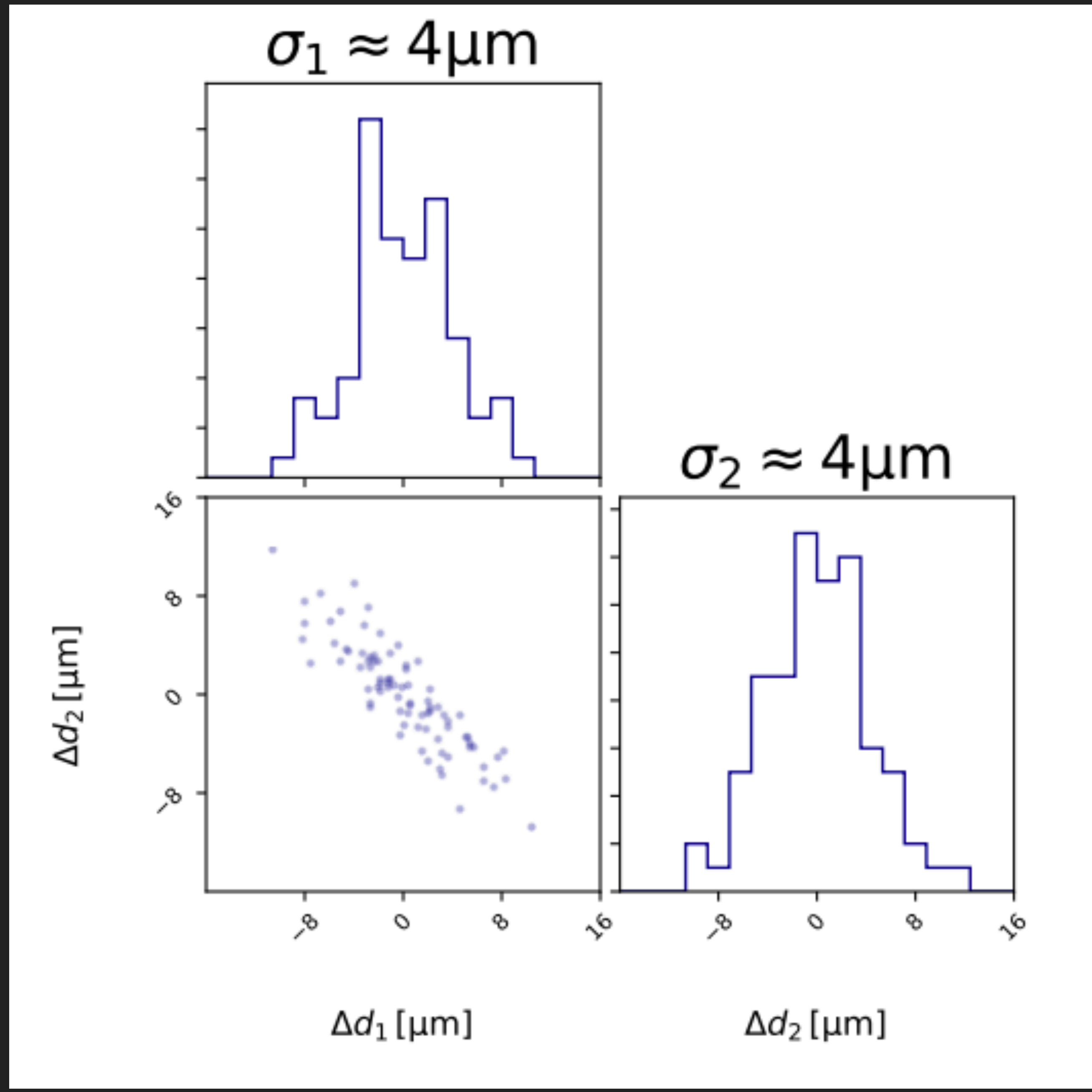

Boost factor uncertainty due to tuning

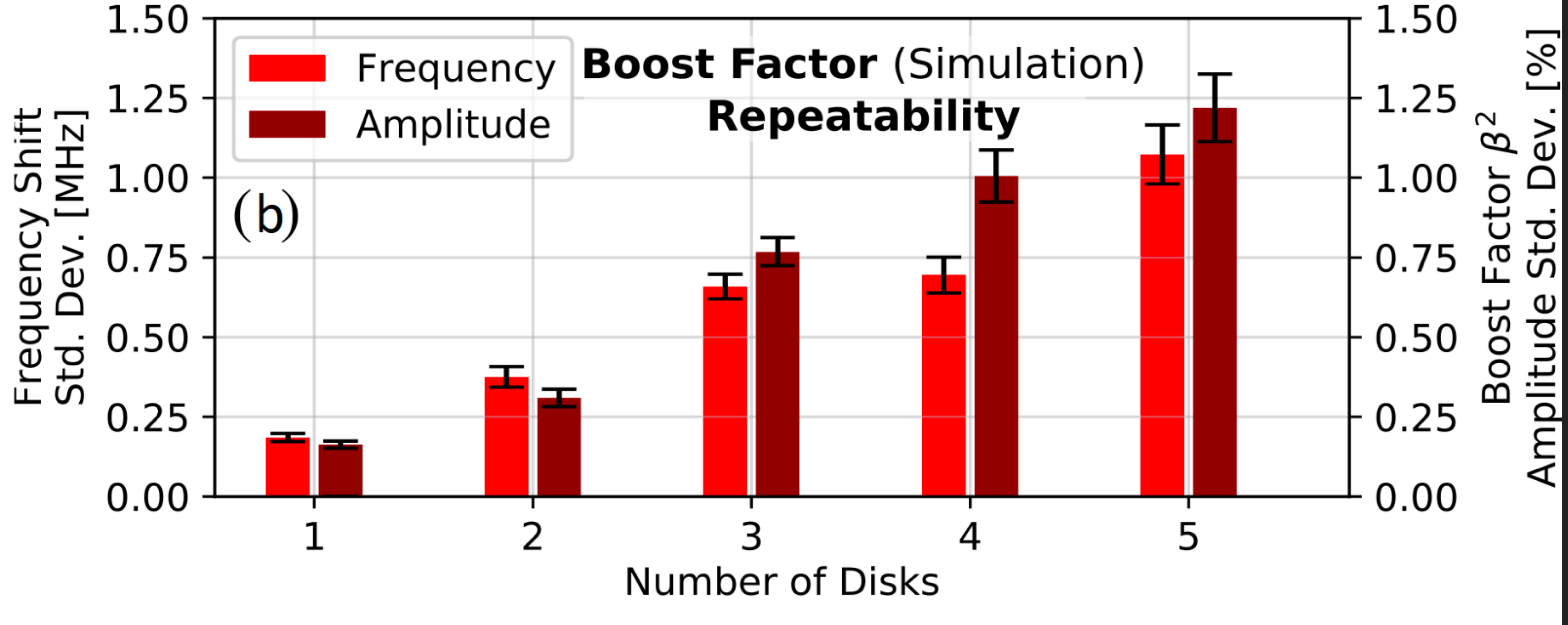

3D EFFECTS: FINITE DISC SIZE

Comsol Multiphysics ®

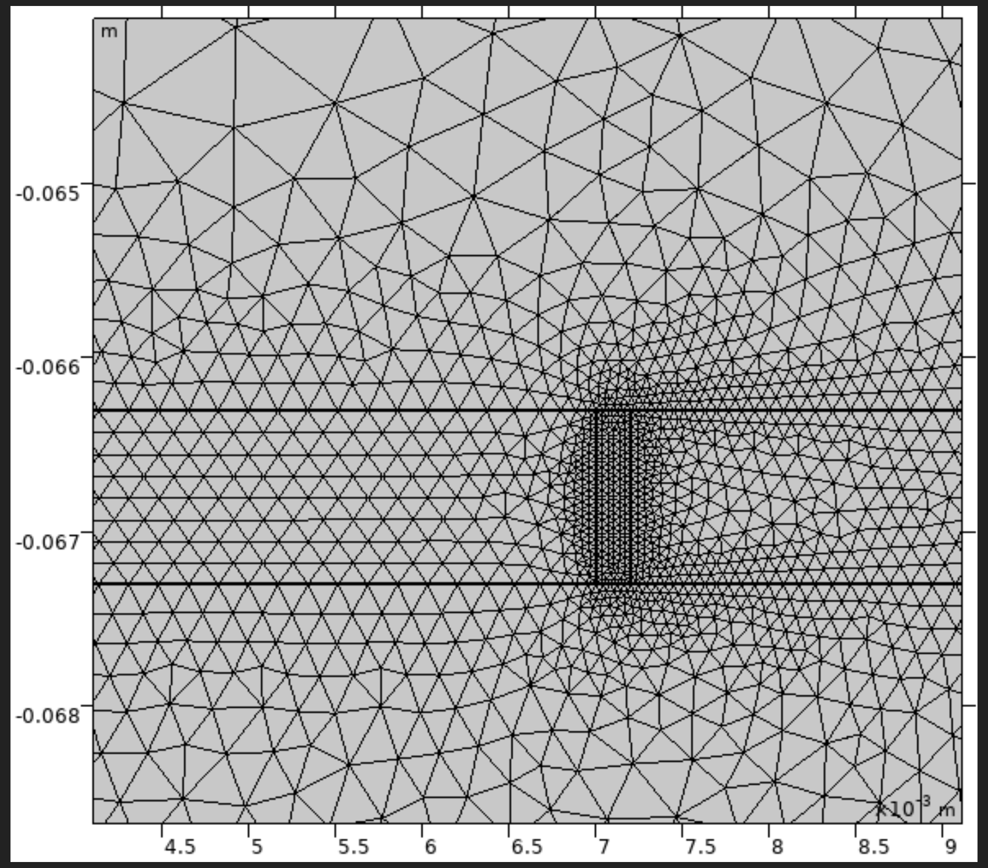

Power boost factor, 20 $LaAlO_3$ discs in free space

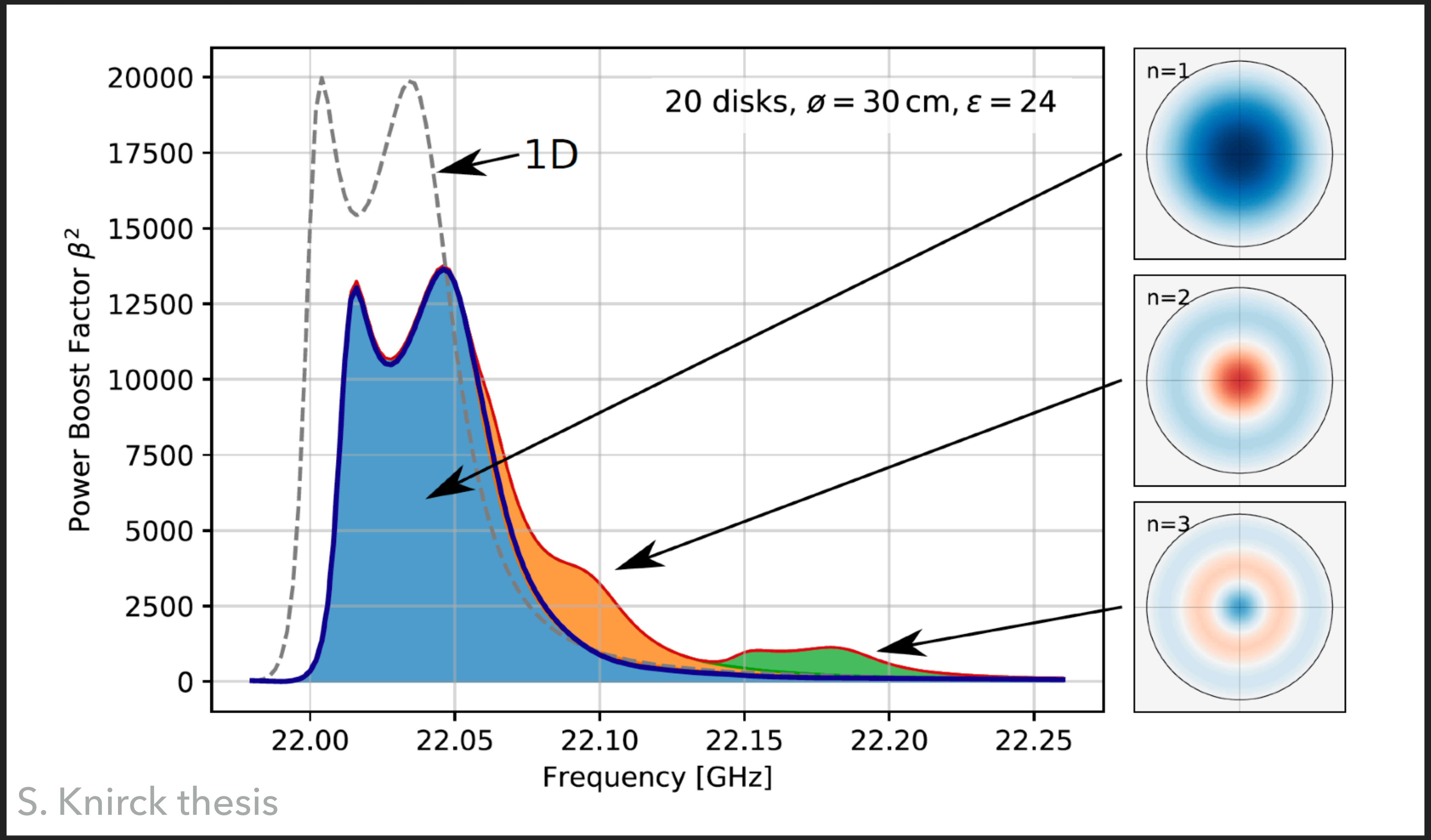

1. Finite Element Method (FEM): a numerical method to solve differential equations
   - Axion-induced source term is implemented as an external current density $\mathbf{J}_a(t) = g_{a\gamma}\mathbf{B}_e\dot{a}(t)$

2. Custom codes using the ray tracing method and the mode matching method are also developed
   - The frequency shift relative to the 1D calculation is due to the difference between the plane wave k and the $k_{||}$'s of the dielectric waveguide
   - Different waveguide modes contribute to the boost factor at different frequencies due to the different $k_{||}$'s

3D EFFECTS: IMPERFECT DISCS

20 discs, $\varnothing = 30$ cm, $\epsilon = 24$

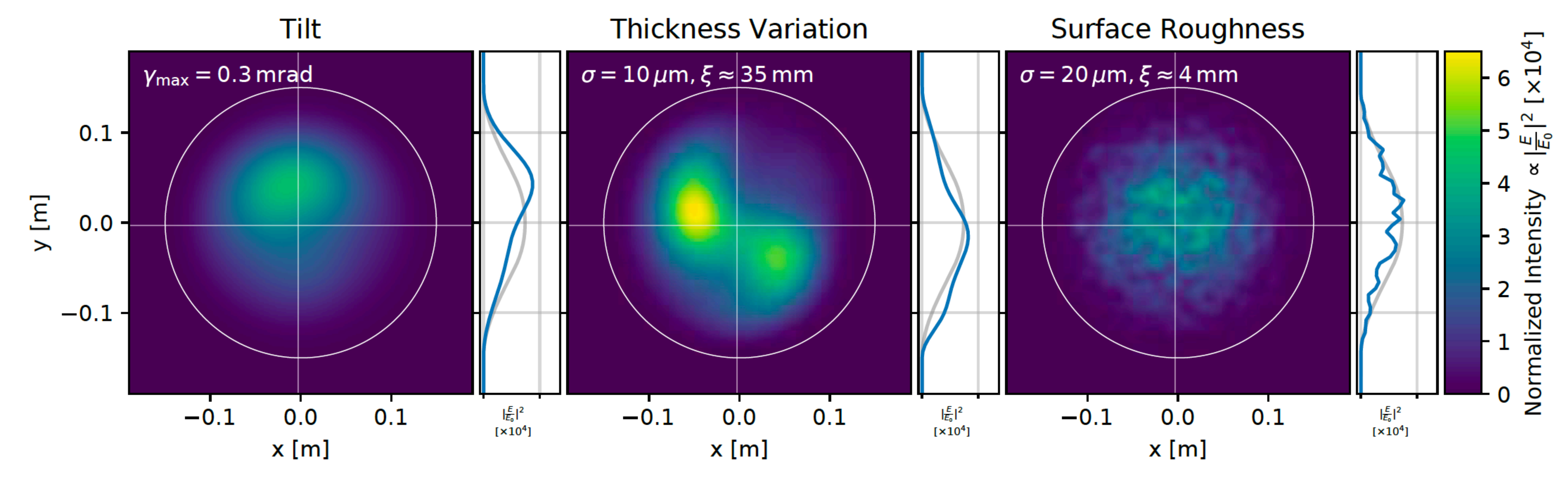

S. Knirck PhD thesis

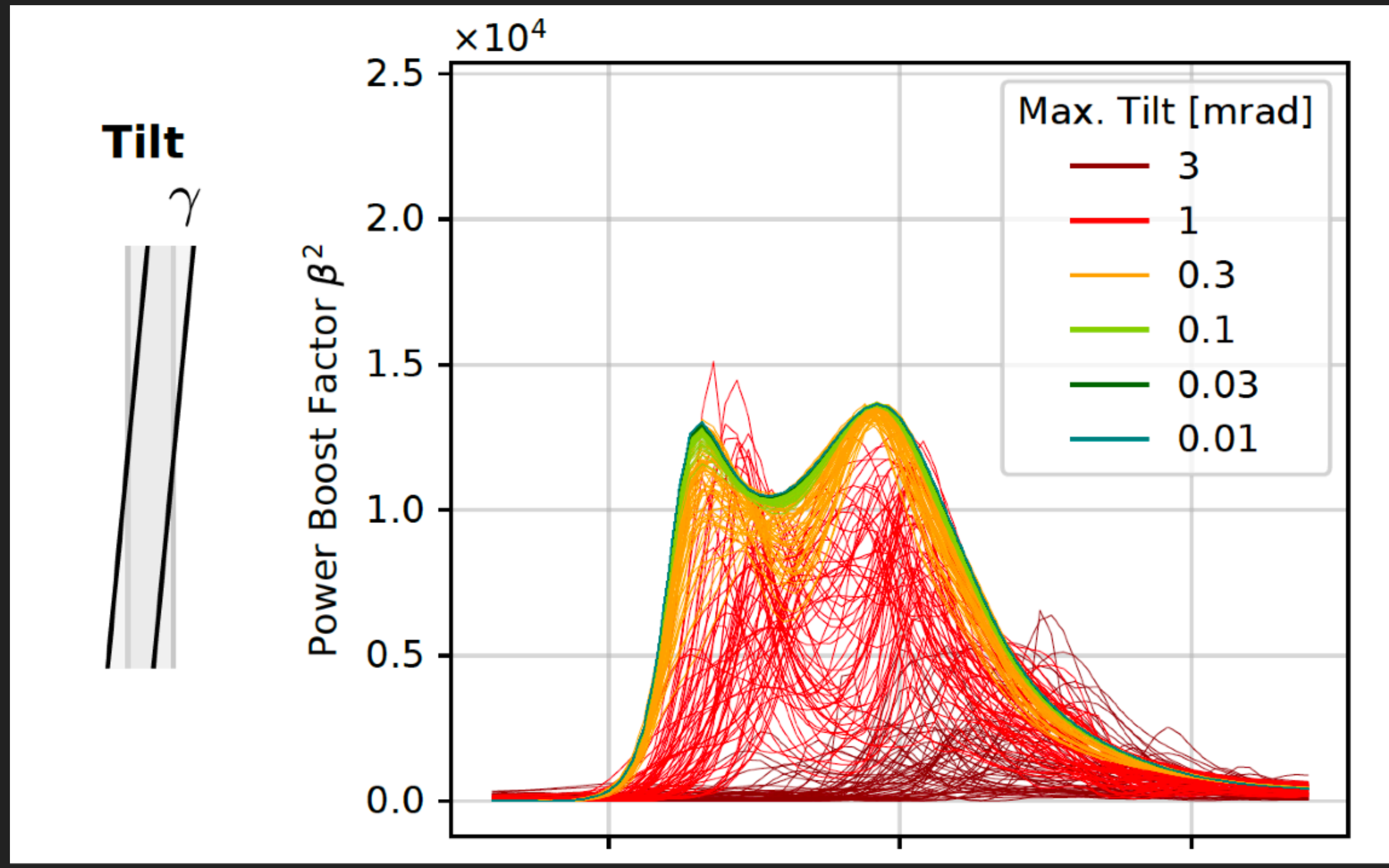

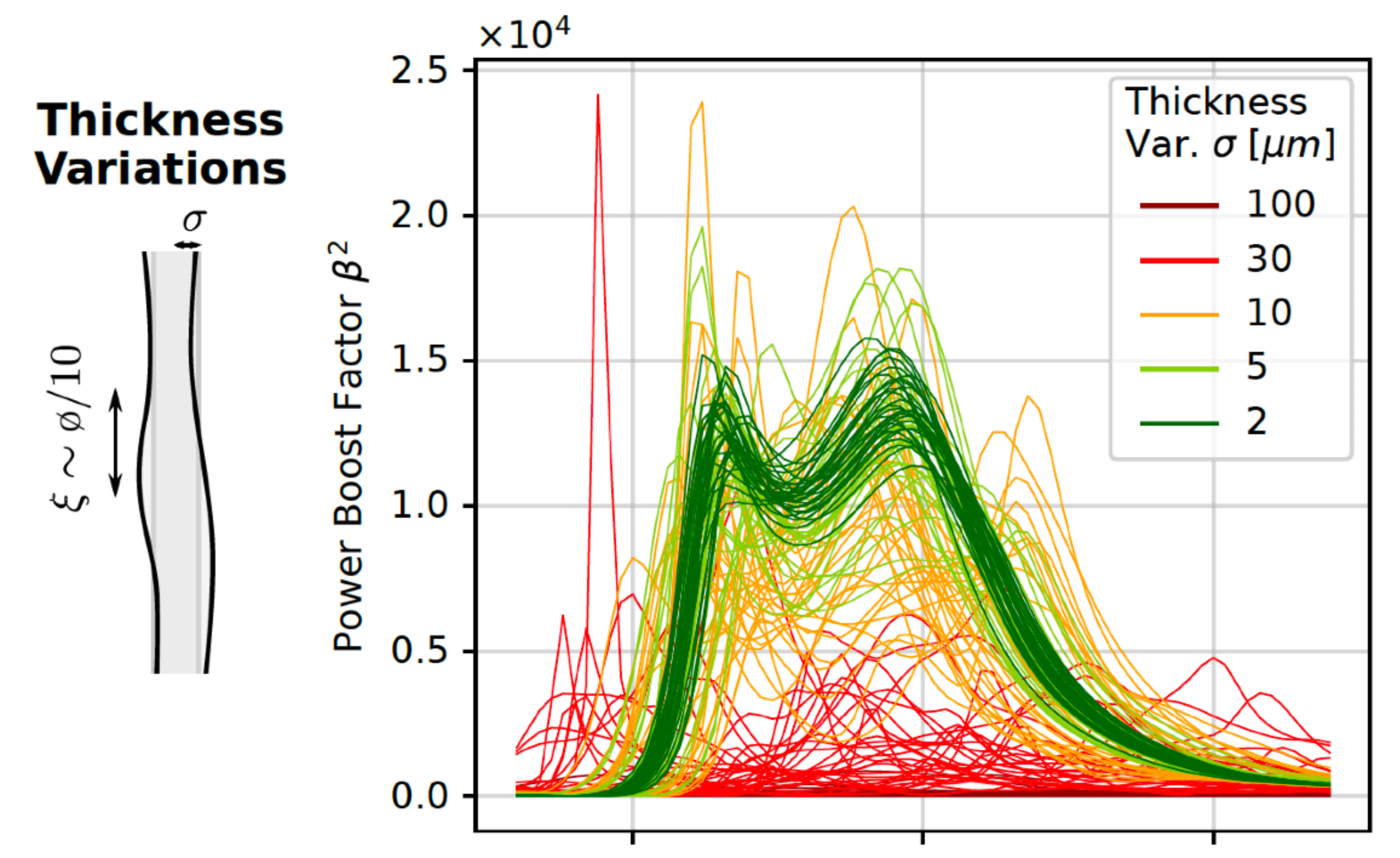

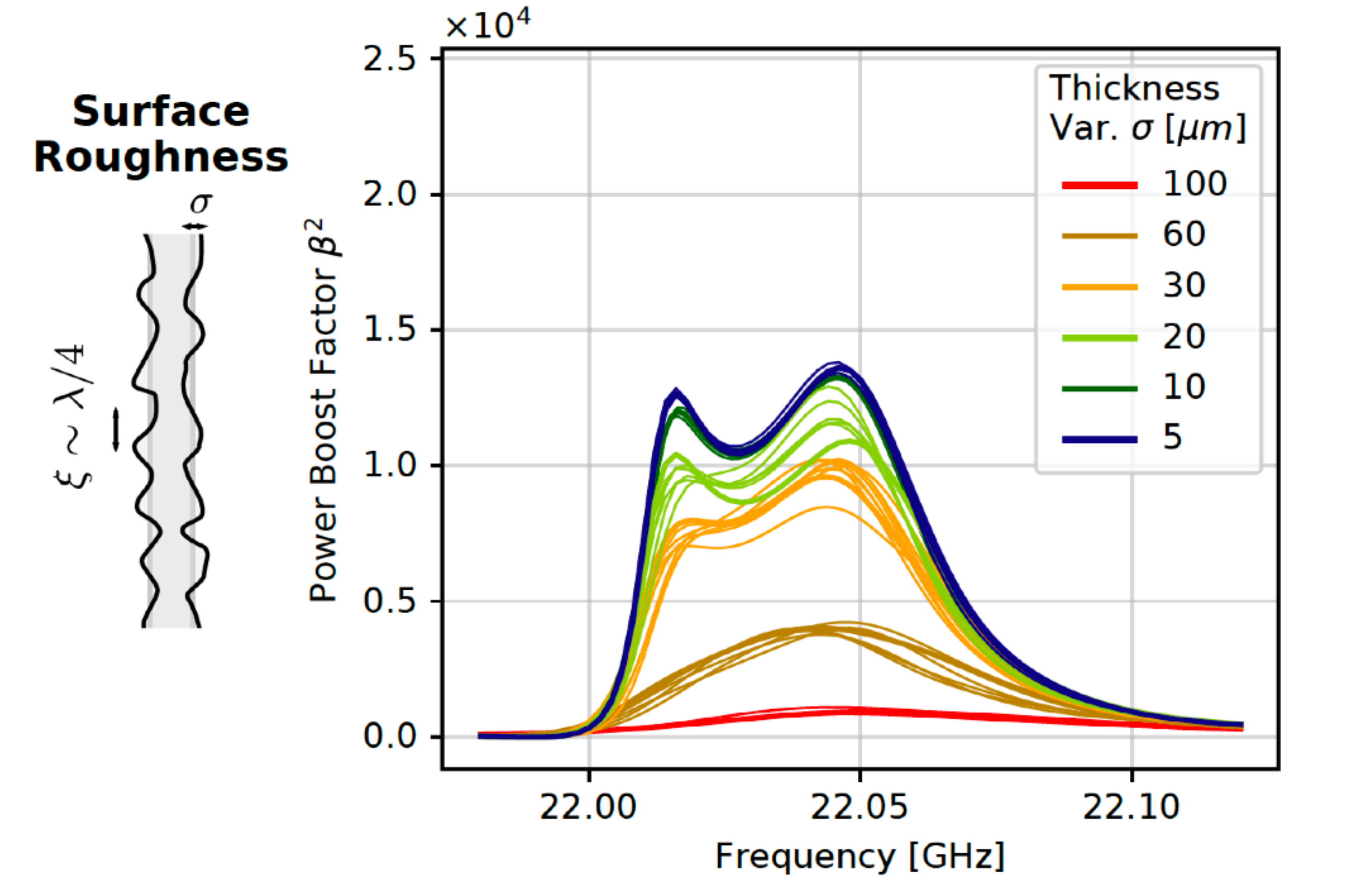

$\gamma \lesssim 0.3$ mrad $\leftrightarrow \Delta z \lesssim 100\ \mu m$

$\sigma \lesssim 5\ \mu m$

Surface roughness less critical

THE RECEIVER

$\sim 10^{-22}$ W fake axion signal detectable with ~2 days of measurement time

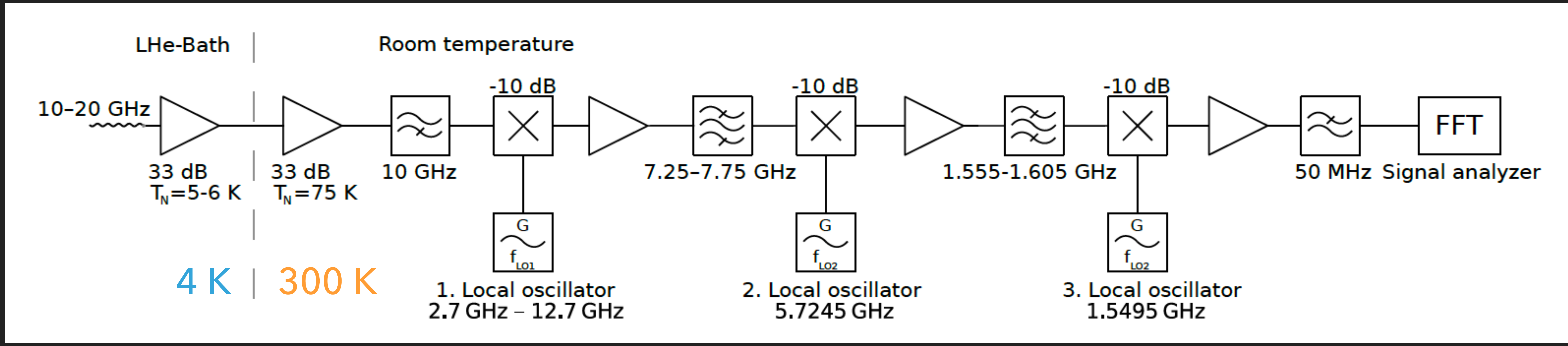

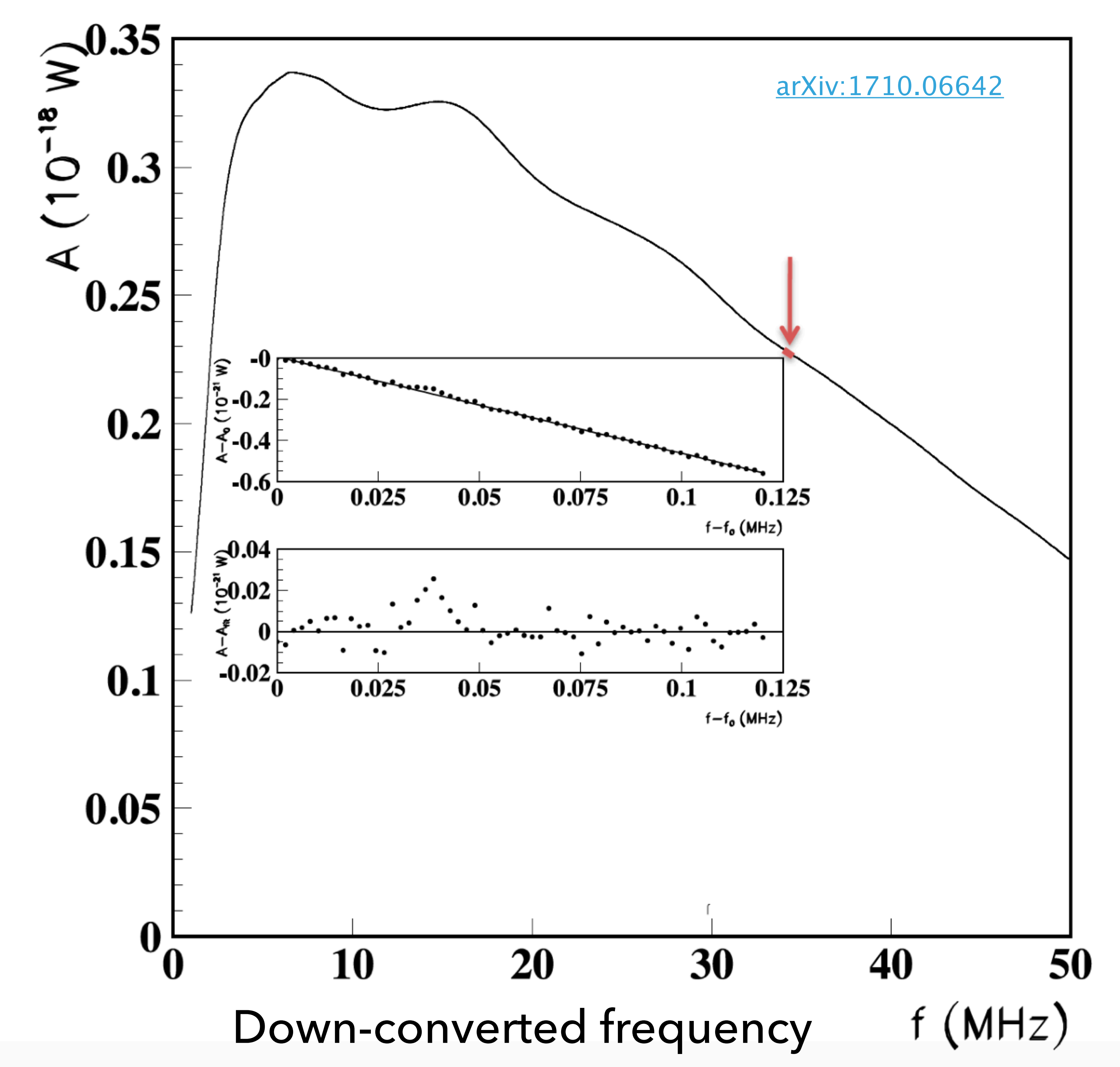

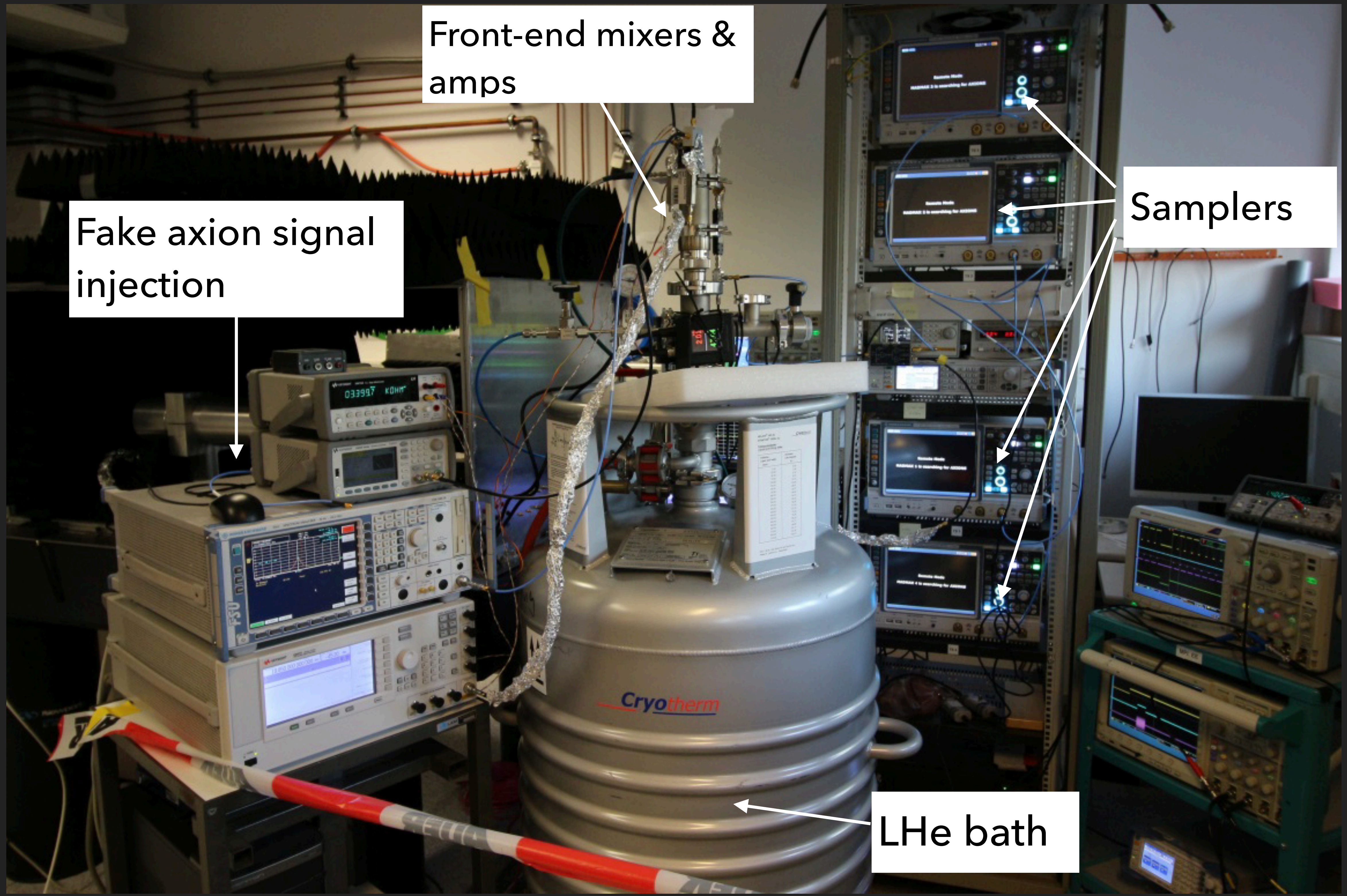

DISC MATERIAL

- Requirements on the discs:
  - Relatively hight ϵ, non-magnetic, low $\tan\delta$ ($\lesssim 10^{-4}$)
  - Can be fabricated/cut in large areas with ~ 1 mm in thickness
  - Sufficient mechanical rigidity

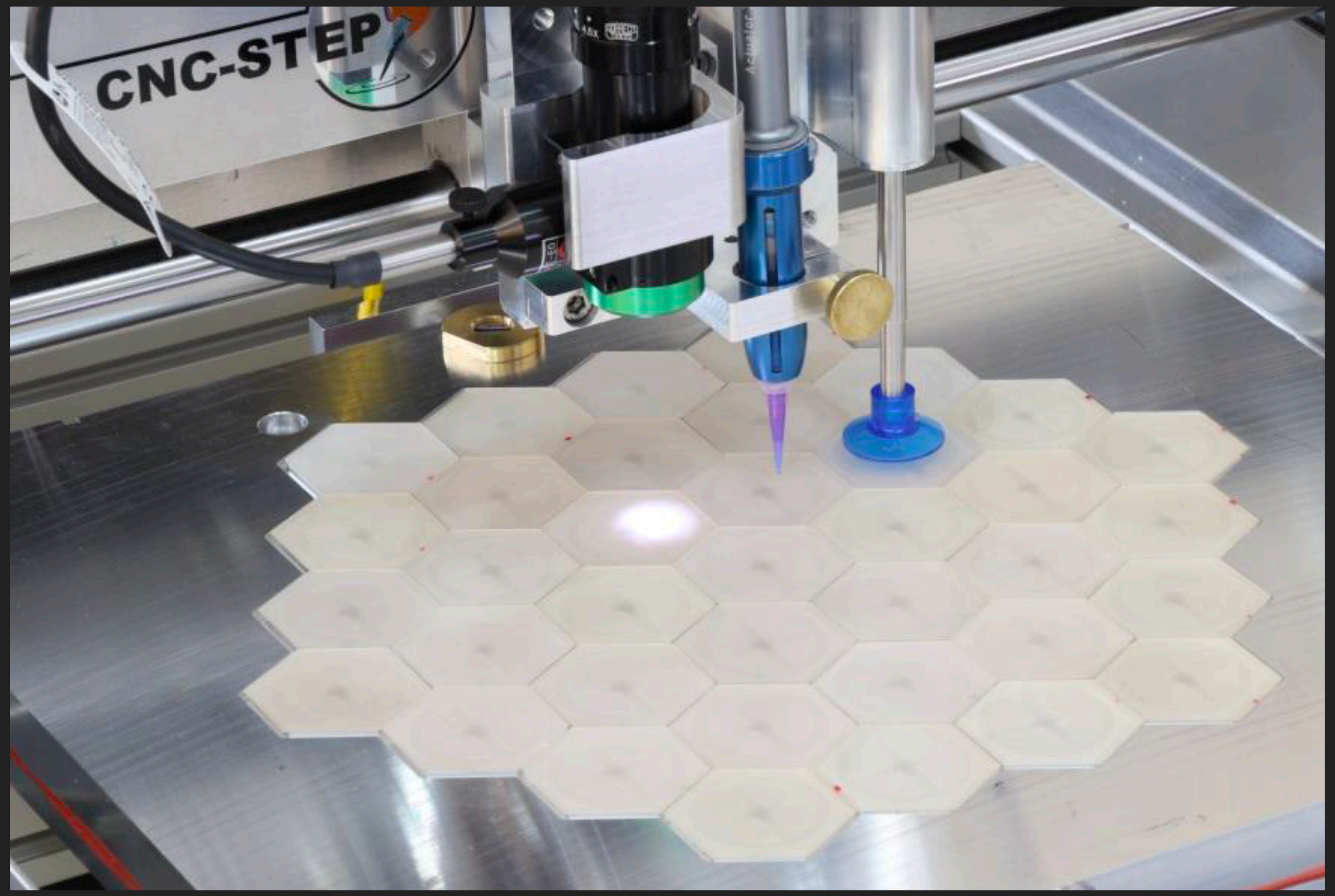

@UHH

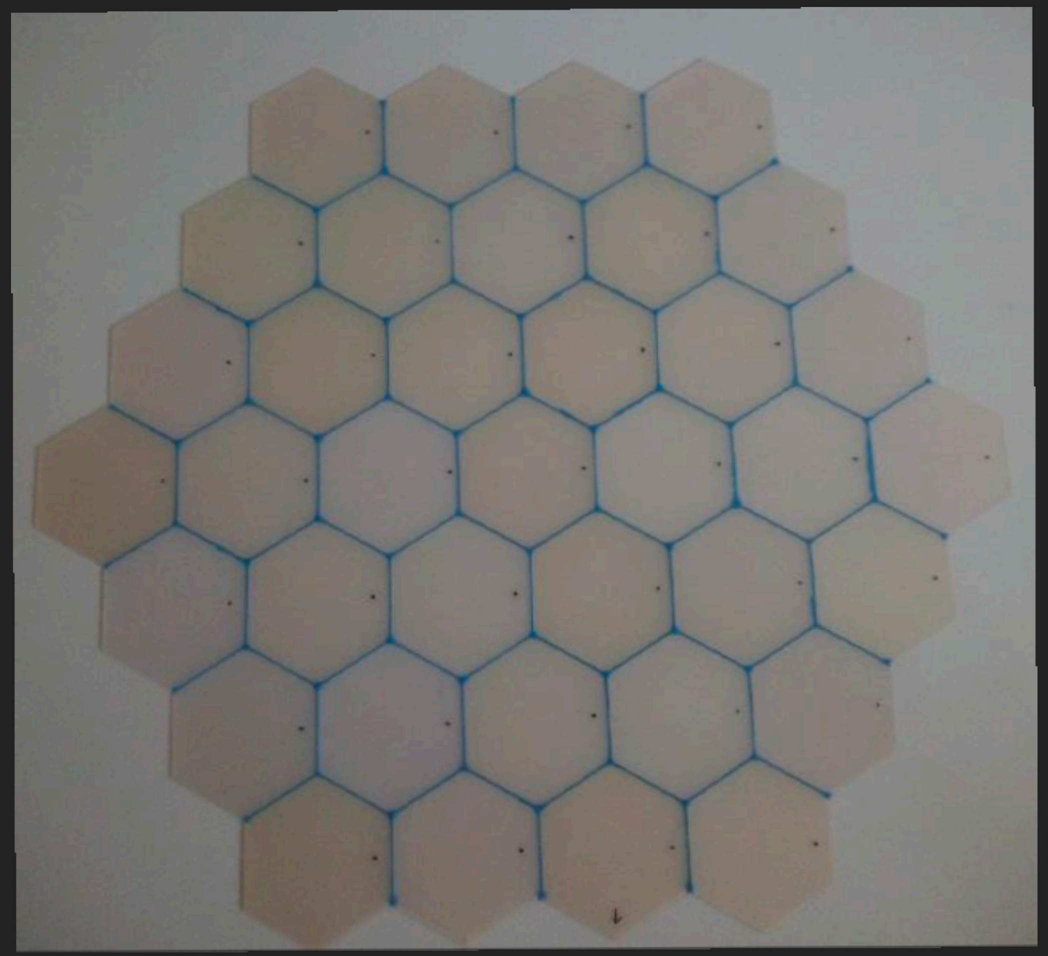

First tiled $LaAlO_3$ disc (Ø 30 cm)

- Candidate materials:
  - $LaAlO_3$
    - $\epsilon \approx 24$
    - $\tan\delta =$ a few $\times 10^{-5}$
    - Only grown on 3″ wafer; tiling needed for 1 m² discs
  - Sapphire
    - $\epsilon \approx 9$ (C-cut)
    - $\tan\delta \approx 10^{-5}$
    - Up to 20″
- Other candidate materials such as alumina are under investigation

DIPOLE MAGNET

Superconducting CICC coil

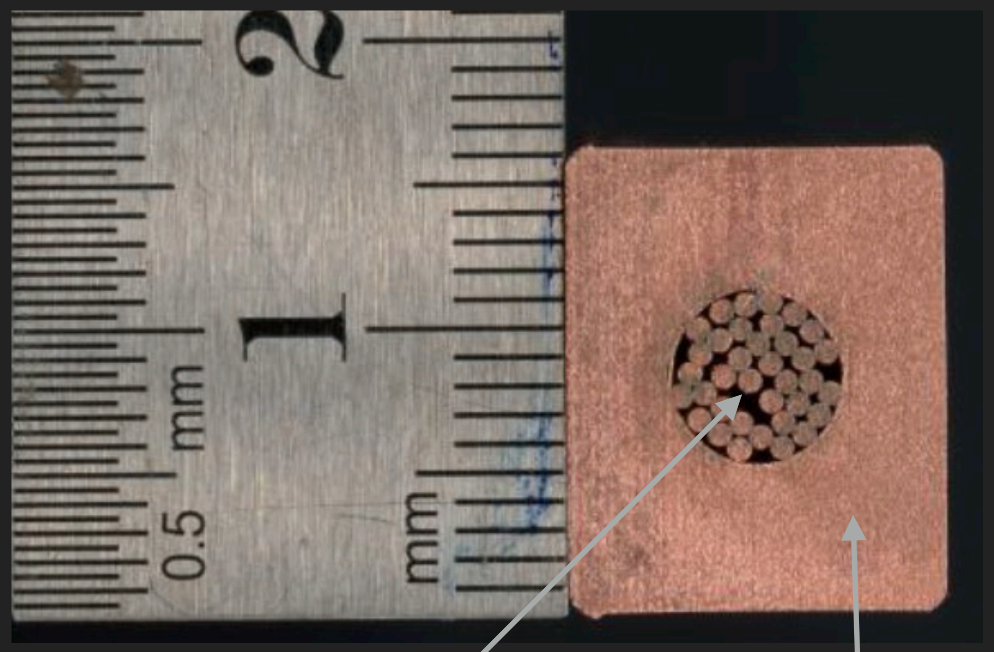

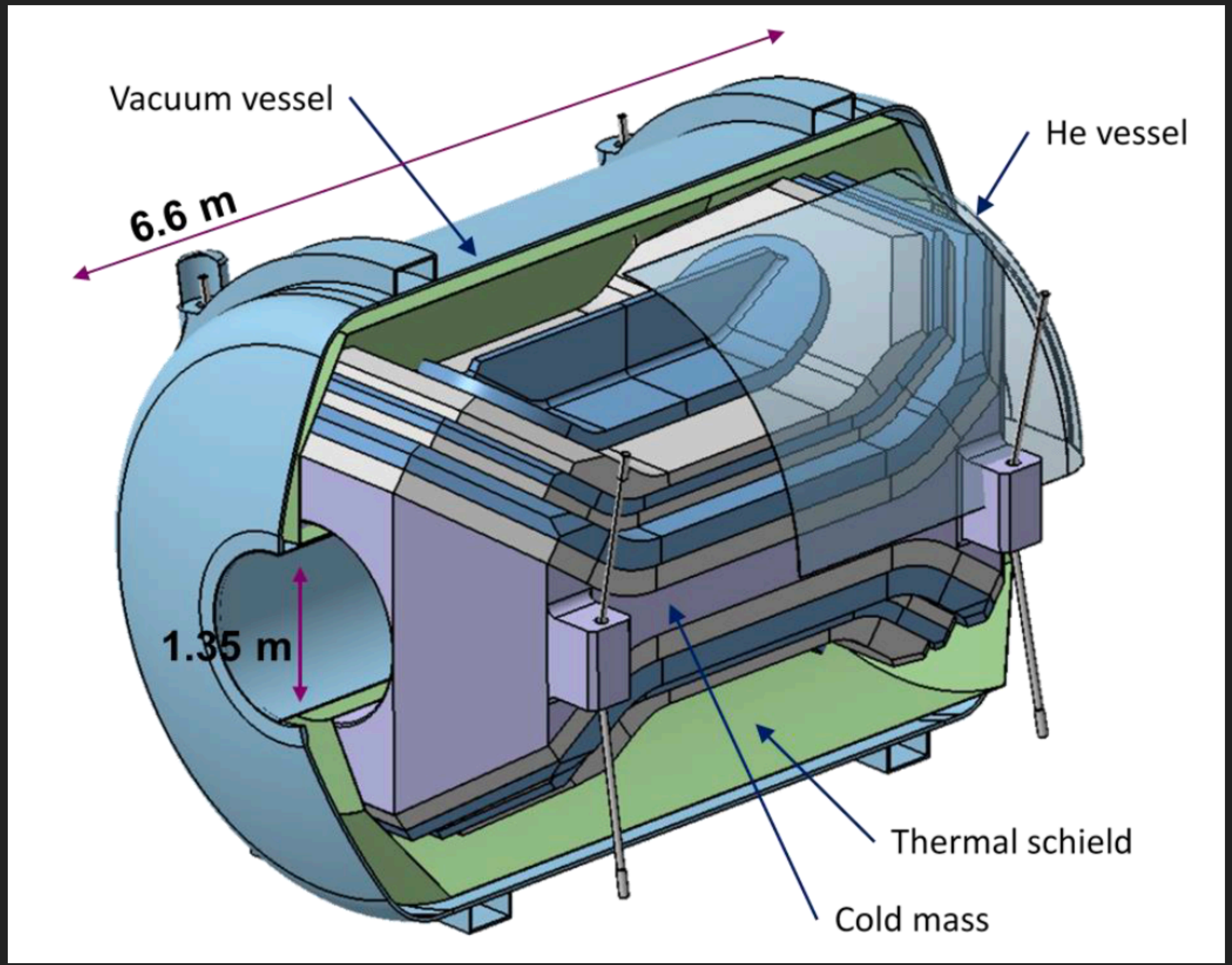

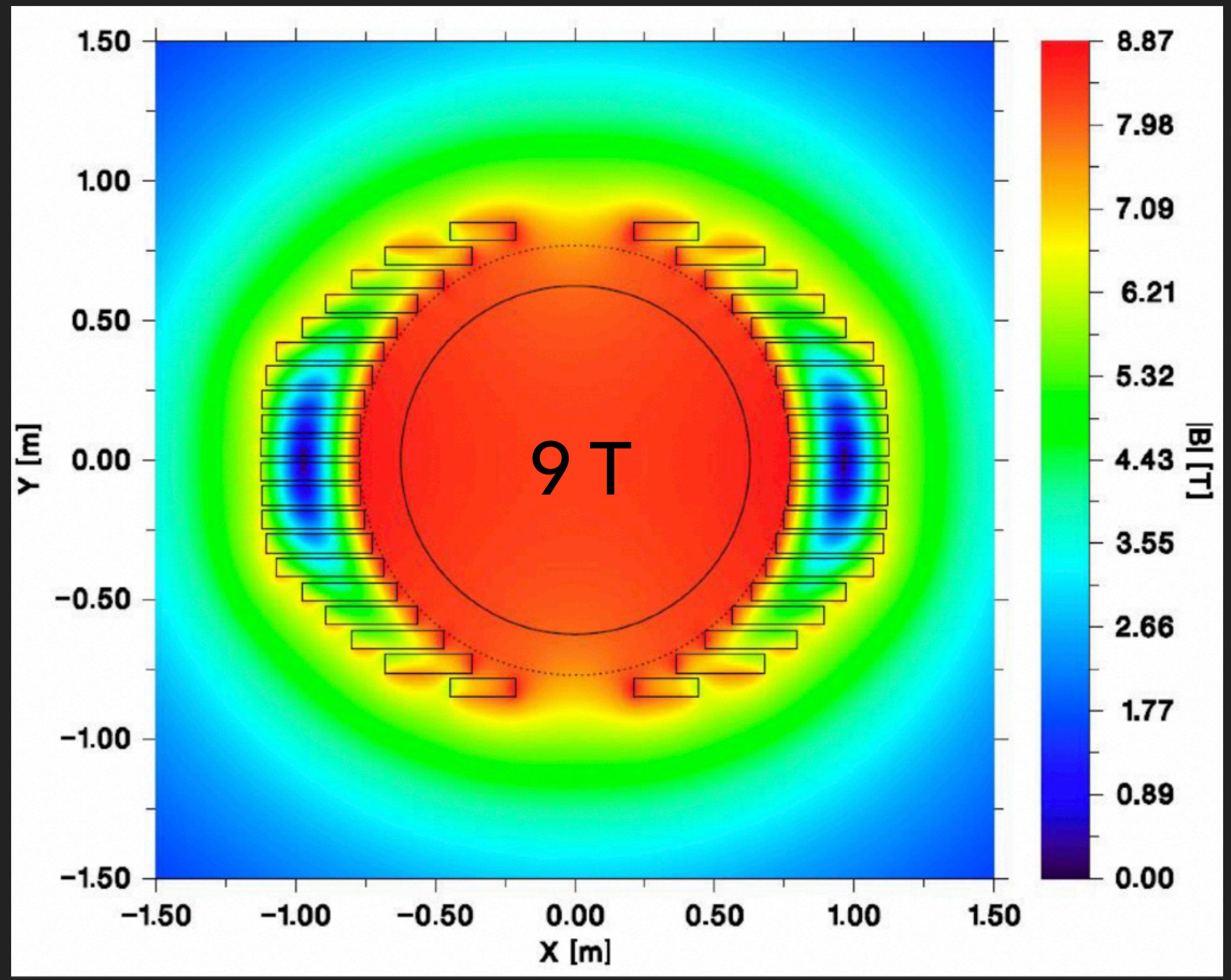

- $B^2 \cdot A \sim 100$ T^{2}m^2 magnet has never been built before
    - NbTi coil, 9 T field, 1.25 m^2 warm bore, highly homogeneous, 480 MJ stored energy
- Partner with CEA Saclay and BILFINGER NOELL GmbH
    - Experience and infrastructure from ITER
    - Quench test with mockup coil soon

MADMAX PROTOTYPE

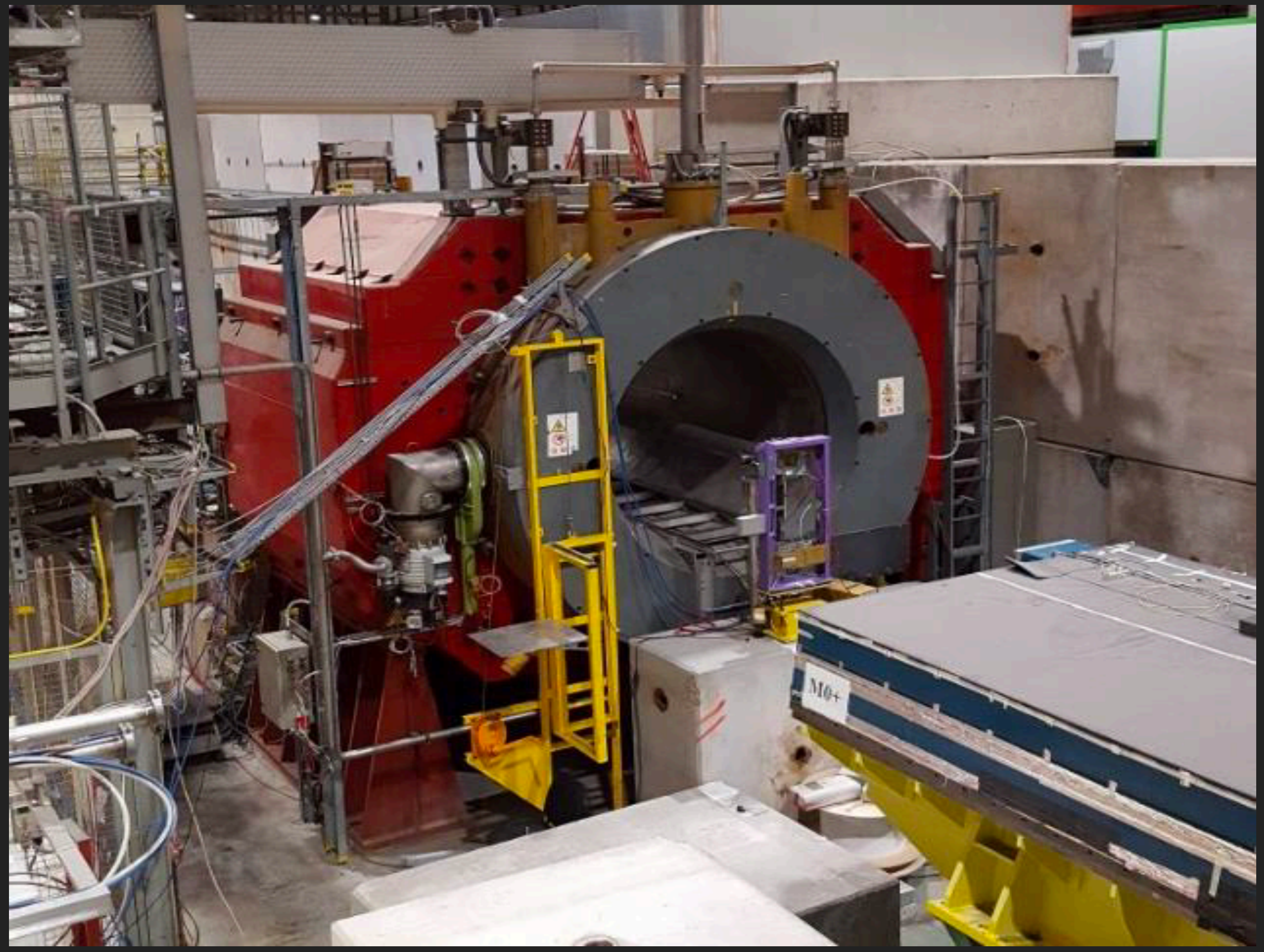

MORPURGO magnet @ CERN

- Prototype detector as an R&D platform
- Plans to use the prototype detector inside the Morpurgo magnet at CERN
  - Hidden photon/ALPs search w/ prototype detector
  - Mechanical test at 1.6 T magnetic field

Cryogenic piezo motor & laser interferometer assembly

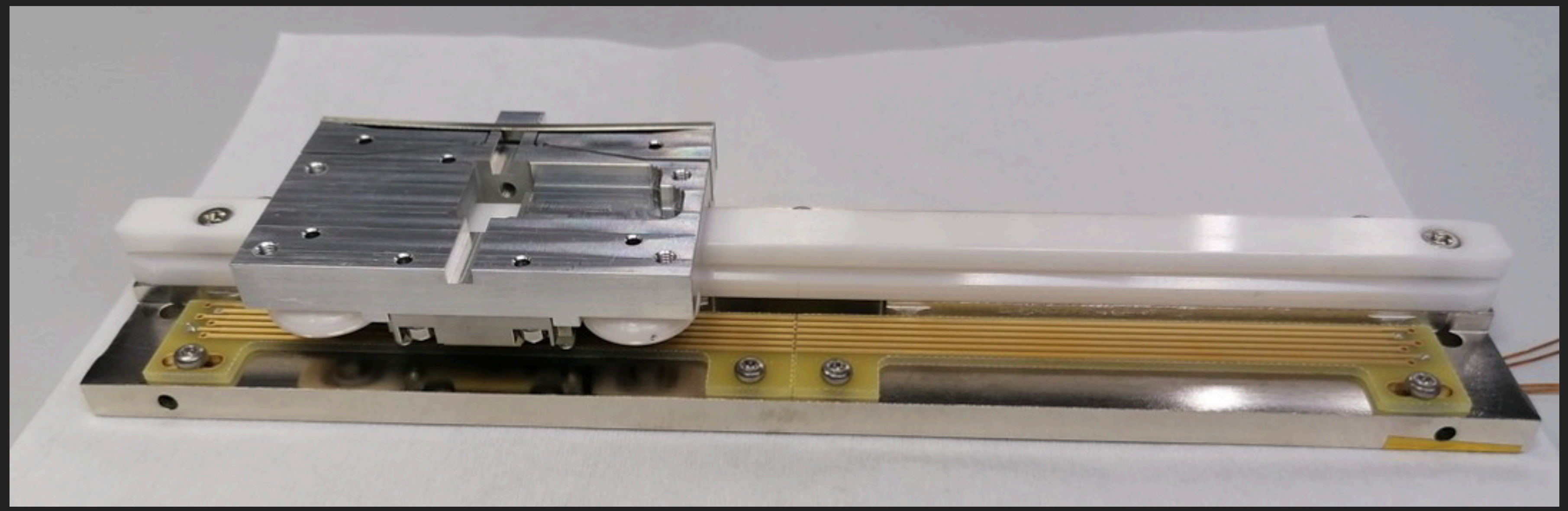

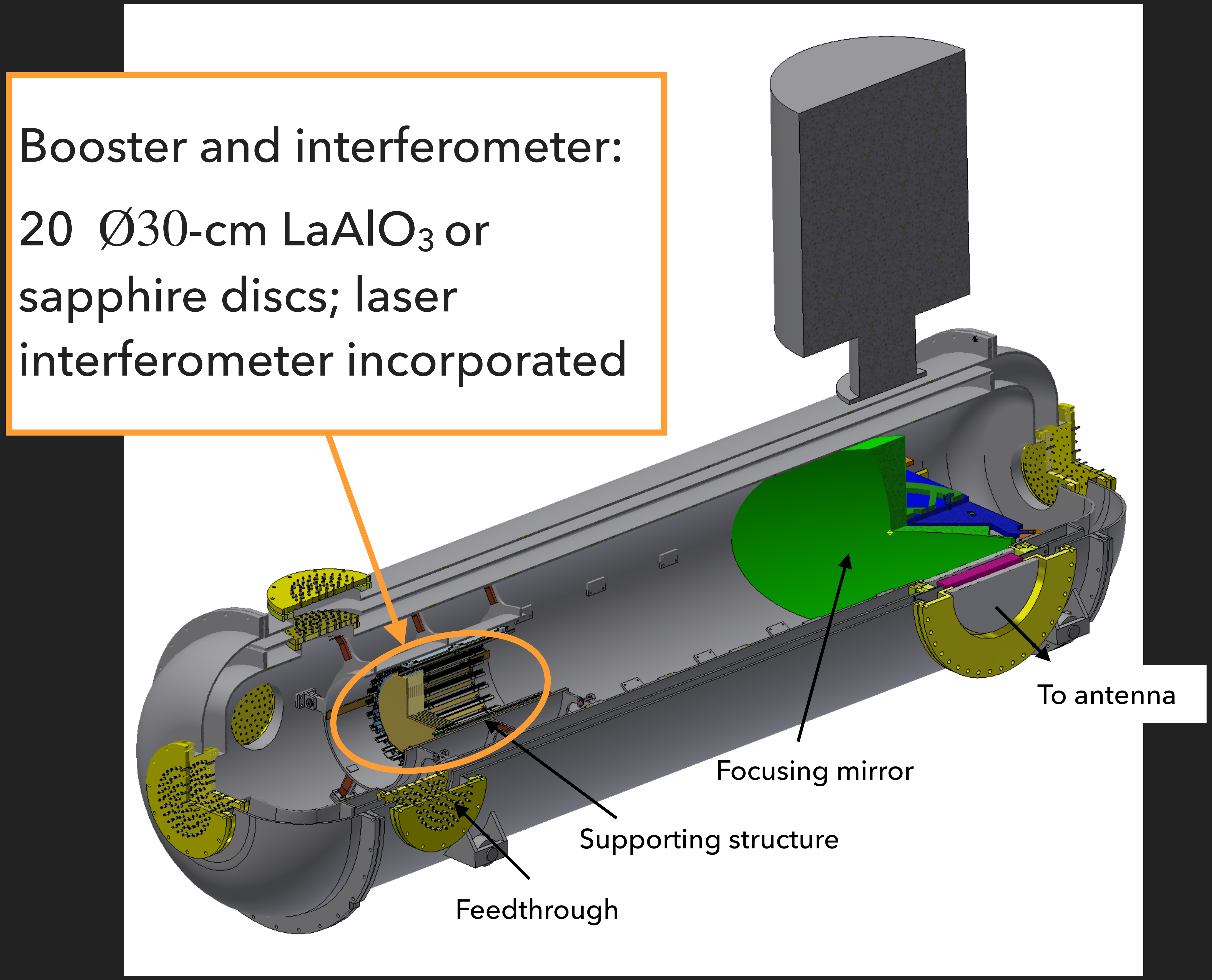

MADMAX PROJECT ROADMAP

2017-2019 DESIGN	2019-2022 PROTOTYPING	2022-2025 PROTOTYPE PHYSICS RUN	202?-2028? MAGNET CONSTRUCTION	2028?- DATA TAKING @ DESY

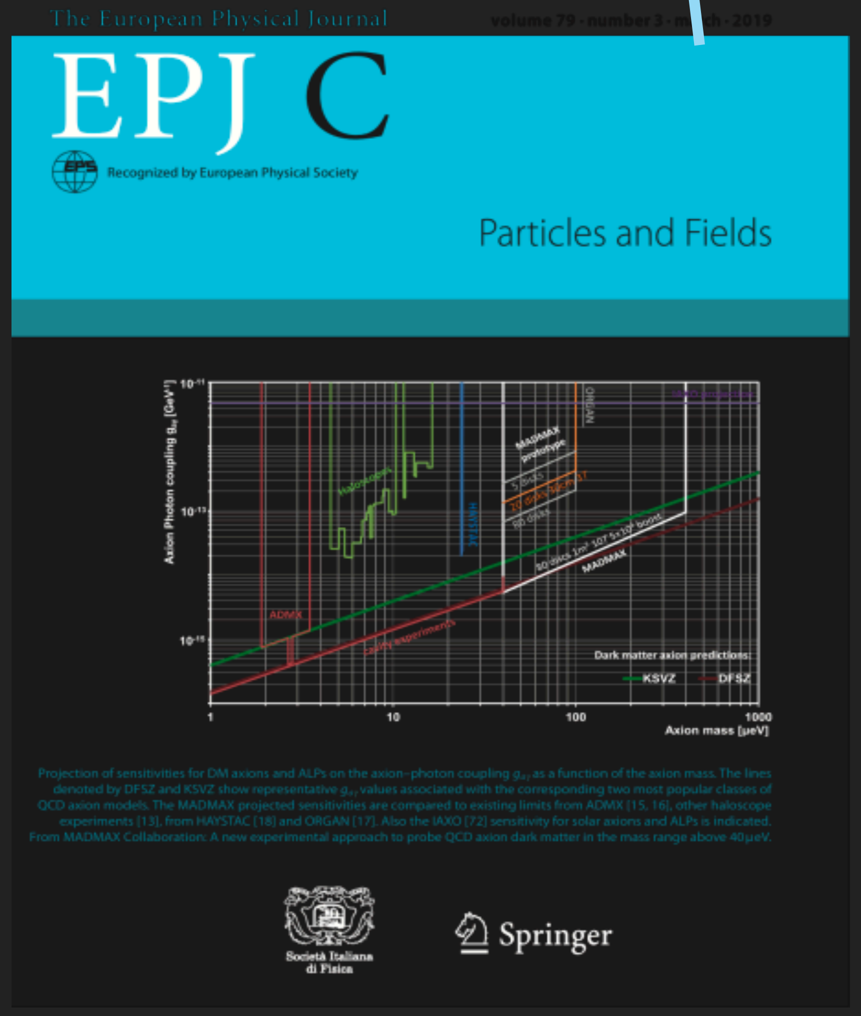

MADMAX white paper

Eur. Phys. J. C (2019) 79: 186

RF lab SHELL @ UHH

MORPURGO magnet @ CERN up to 1.6 T

Prototype detector data taking

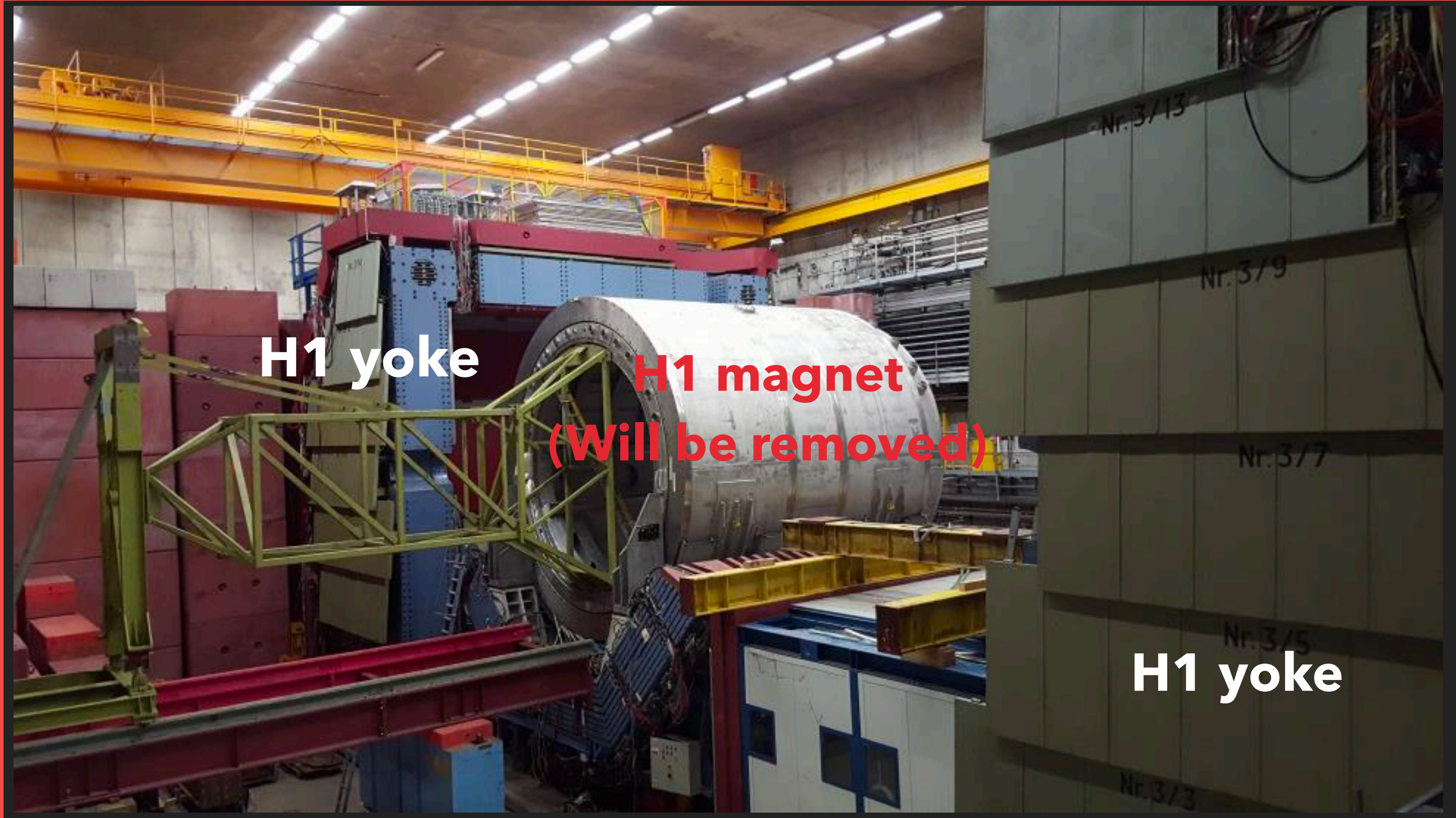

w/ full-sized detector and 9T magnet at DESY HERA Hall North

MADMAX SENSITIVITY

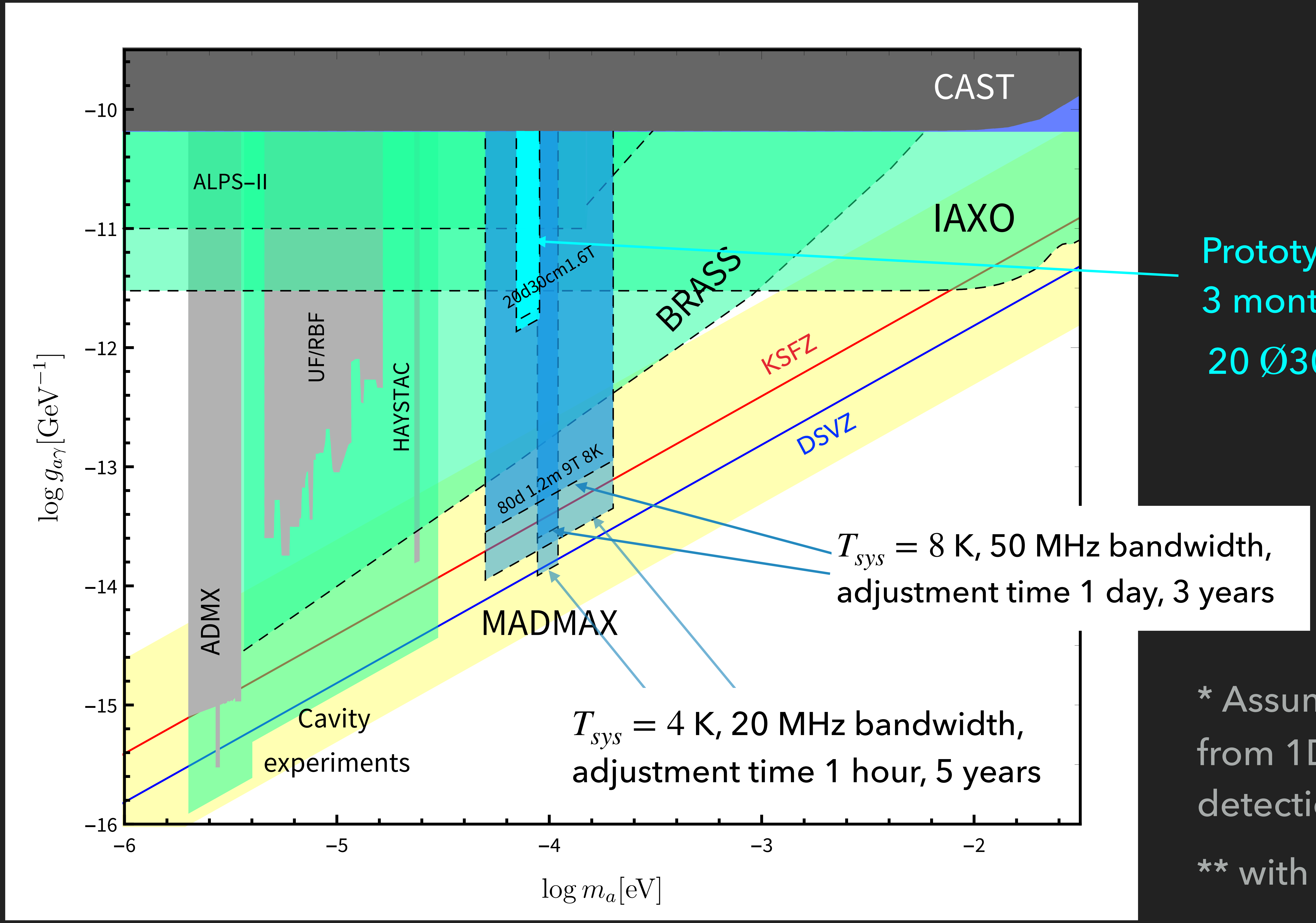

* Assuming 50% of obtainable power from 1D simulation is received; 5σ detection level

** with $100\ \mathrm{T}^2\mathrm{m}^2$ magnet

THANK YOU!